nagra

National Cooperative for the
Disposal of Radioactive Waste

TECHNICAL REPORT 94-03

Modelling of the Near-Field Chemistry of the SMA Repository at the Wellenberg Site: Application of the Extended Cement Degradation Model

October 1994

F. Neall

PSI, Würenlingen and Villigen

Hardstrasse 73, CH-543o Wettingen/Switzerland, Telephone +41-56-37 11 11

nagra National Cooperative for the Disposal of Radioactive Waste

TECHNICAL REPORT 94-03

Modelling of the Near-Field Chemistry of the SMA Repository at the Wellenberg Site:

Application of the Extended Cement Degradation Model

October 1994

F. Neall

PSI, Würenlingen and Villigen

Hardstrasse 73, CH-543o Wettingen/Switzerland, Telephone +41-56-37 11 11

This report was prepared on behalf of Nagra. The viewpoints presented and conclusions reached are those of the author(s) and do not necessarily represent those of Nagra.

Preface

In the framework of its Waste Management Programme the Paul Scherrer Institute is performing work to increase the understanding of repository near-field behaviour. These investigations are performed in close cooperation with, and with the financial support of NAGRA. The present report is therefore issued simultaneously as a PSI report and as a NAGRA NTB.

ABSTRACT

Of the materials which make up the L/ILW repository for short-lived low- and intermediate-level wastes, around 95 weight percent consists of concrete, around 4% of steel and around 1% of high molecular weight organic waste components. In this report, models are used to evaluate the long-term stability of concrete, steel and high molecular weight organic components under repository conditions. The results of this study will then form the basis for describing release of radionuclides from the disposal caverns, and particularly the sorption of nuclides on concrete.

In the disposal caverns, concrete is exposed to a range of processes which affect its stability. External processes include the leaching of hydrated cement by percolating groundwater, while internal processes include dissolution of repository components in cement porewater which can then react with the concrete. Of greatest significance in this respect are the high molecular weight organic waste components which degrade to organic acids in the disposal environment and then react with the basic components of the concrete.

The leaching of hydrated cement is described, using a mixing tank model, as a sequence of batch experiments in which the same cement block reacts repeatedly with fresh groundwater. The model is based on the work by Berner (1990) but has been extended to include other solid cement phases and can, in a simple way, take account of the degradation of high molecular weight organics and their reaction with hydrated cement. The mixing tank model shows that, given the low water fluxes that are expected for a L/ILW repository, concrete remains stable over geological time spans provided only small volumes of high molecular weight organics are present. If high concentrations of these materials are present, the longevity of the concrete may be reduced.

The redox conditions in the disposal caverns are determined mainly by the corrosion of steel. In the first decades following repository closure (aerobic phase), corrosion processes consume the oxygen present in the repository until only traces are left. Once the oxygen has been consumed, anaerobic corrosion of steel and other metal components takes place over several thousands of years; the redox conditions during this phase are strongly reducing. Once all the metals in the repository have corroded, the redox state will adjust gradually to that of the inflowing groundwater.

ZUSAMMENFASSUNG

Das Endlager SMA für kurzlebige schwach- und mittelaktive Abfälle besteht zu ca. 95 Gewichtsprozent aus Beton, zu ca. 4 % aus Stahl und zu ca. 1% aus hochmolekularen organischen Abfallkomponenten. Im vorliegenden Bericht wird die langfristige Beständigkeit von Beton, Stahl und hochmolekularen organischen Abfallkomponenten unter Endlagerbedingungen in Abhängigkeit der Zeit modellhaft beurteilt. Dies ist Grundlage für die Beschreibung der Freisetzung von Radionukliden aus den Endlagerkavernen, im besonderen der Sorption von Radionukliden an Beton.

In den Endlagerkavernen wirken verschiedene Prozesse auf Beton ein, die seine Beständigkeit beeinflussen. Von aussen ist dies die Auslaugung von Zementstein durch das durchströmende Grundwasser. Von innen ist dies die Auflösung von Endlagerkomponenten in das Zementporenwasser, welche mit Beton reagieren können. Hierfür am bedeutendsten sind die hochmolekularen organischen Abfallkomponenten, die unter Endlagerbedingungen zu organischen Säuren abgebaut werden und mit den basischen Komponenten von Beton reagieren.

Die Auslaugung von Zementstein wurde durch ein Mischbehältermodell als eine Abfolge von Batch-Experimenten beschrieben, in denen der gleiche Zementblock immer wieder mit frischem Grundwasser reagiert. Das Mischbehältermodell beruht auf Berner (1990). Es wurde durch weitere Zementfestphasen erweitert und kann vereinfacht die Degradation von hochmolekularen Organika und ihre Reaktion mit Zementstein berücksichtigen. Das Mischbehältermodell zeigt, mit den geringen Wasserflüssen wie sie für ein SMA-Endlager vorgesehen sind, dass Beton über geologische Zeiträume beständig ist, wenn hochmolekulare Organika in kleinen Mengen vorhanden sind. Bei hohen Gehalten an hochmolekularen Organika kann die Beständigkeit von Beton jedoch herabgesetzt sein.

Der Redoxzustand der Endlagerkavernen wird vor allem durch die Korrosion von Stahl bestimmt. In den ersten Jahrzehnten nach Endlagerverschluss (aerobe Phase) wird der Sauerstoff im Endlager durch die Korrosionsvorgänge bis auf Spuren aufgebraucht. Nach Abbau des Sauerstoffs findet während einiger Jahrtausende die anaerobe Korrosion des Stahls und der anderen Metallbestandteile statt. Der Redoxzustand ist während dieser Phase stark reduzierend. Nachdem alle Metalle im Endlager korrodiert sind, passt sich der Redoxzustand langsam dem des einfliessenden Grundwassers an.

RESUMÉ

Le dépôt final pour déchets de faible et moyenne activité à vie courte (DFMA) contient en poids environ 95% de béton, env. 4% d'acier et env. 1% de déchets constitués de composés organiques de poids moléculaires élevés. Le présent rapport évalue la tenue à long terme du béton, de l'acier et des composants de déchets organiques de poids moléculaires élevés, dans les conditions prévalant dans un dépôt final, à l'aide de modèles en fonction du temps. Ceci constitue la base de la description du relâchement de radionucléides des cavernes de stockage et notamment de la sorption de radionucléides sur le béton.

Divers phénomènes affectant la tenue du béton se déroulent dans les cavernes de stockage final. De l'extérieur ce sera la lixiviation de la pierre de ciment par la circulation d'eau souterraine. De l'intérieur ce sera la dissolution, dans l'eau intersticielle du ciment, de composants de déchets qui peuvent réagir avec le béton. Parmi ceux-ci les plus significatifs sont les composants de déchets organiques de poids moléculaires élevés qui dans les conditions régnant dans un dépôt final se désintègrent en acides organiques et réagissent avec les composants basiques du béton.

La lixiviation de la pierre de ciment a été décrite par un modèle de mélangeur, sous forme d'une suite d'expériences par lots, dans lesquelles le même bloc de ciment réagit constamment à nouveau avec de l'eau souterraine fraîche. Ce modèle de mélangeur se fonde sur Berner (1990). Il a été élargi à de nouvelles phases du ciment et peut de façon simplifiée tenir compte de la dégradation de substances organiques de poids moléculaires élevés et de leurs réactions avec la pierre de ciment. Le modèle de mélangeur montre, qu'avec les faibles apports d'eau prévus dans un dépôt final DFMA, le béton résiste durant des temps géologiques lorsque des substances organiques de poids moléculaires élevés sont présentes en faibles quantités. Pour des teneurs importantes de substances organiques de poids moléculaires élevés la résistance du béton peut toutefois diminuer.

L'état rédox des cavernes de stockage final est essentiellement déterminé par la corrosion de l'acier. Durant les premières décennies suivant la fermeture du dépôt final (phase aérobie), l'oxygène présent dans le dépôt est, à quelques traces près, totalement consommé par les phénomènes de corrosion. Après disparition de l'oxygène apparaît, durant quelques milliers d'années, la corrosion anaérobie de l'acier et d'autres composants métalliques. L'état rédox est fortement réducteur durant cette phase. Après corrosion totale de tous les métaux du dépôt final, l'état rédox sera lentement ajusté à la condition réductrice des apports d'eau souterraine.

CONTENTS

LIST OF FIGURES

LIST OF TABLES

1 INTRODUCTION

Cement and concrete (i.e. cement plus aggregate material such as quartz sand) form the main part of the engineered barrier system in the planned Swiss low- and intermediate-level radioactive (SMA) waste repository. Thus, with steel, they constitute the major part of the near field. The accessibility of cement to groundwater means that it will have great influence on the chemical environment of the repository. (Concrete also provides a physical barrier. However, because of the favourable Wellenberg geosphere (low hydraulic conductivity, small hydraulic head), this rôle is of secondary importance and is not discussed here.)

The good sorption properties of cement for many radionuclides constitute an important factor in delaying and decreasing their release into the far field: as a consequence of the low radionuclide inventories planned for this repository, radionuclide releases are probably not solubility-controlled. Sorption is dependent on the degradation state of the cement and on the redox conditions (see BRADBURY & SAROTT 1994). From experiments, the degradation behaviour of cement in water has been determined and may be described qualitatively as having three distinct stages:

I) Non-equilibrium dissolution of the alkali hydroxides (NaOH and KOH) resulting in an initially high pH, commonly in excess of 13.5, which falls rapidly to around 12.5 as these phases are exhausted;

II) The slow fall of pH from 12.5 to around 11.0 as portlandite dissolves followed by the dissolution of the calcium-silicate-hydrate (CSH) gel phase;

III) The rapid fall of pH from around 11.0 as the pH buffering capacity of the CSH gel is exhausted, and other cement phases, hydrogarnet, ettringite and hydrotalcite, dissolve.

Sorption is expected to be greater in stages I and II (BRADBURY & SAROTT 1994), than in stage III. For all stages, it is also expected that sorption for the safety-relevant elements under reducing conditions is equal to or greater than for oxidising conditions. The duration of stages I and II is dependent on several factors including the starting cement composition, composition of the leaching solution or groundwater and rate of water flow. This report describes an attempt to quantify the duration of the high pH conditions (stages I and II) for safety analysis (transport of nuclides) by chemical modelling of the degradation of cement. The evolution of Eh conditions in the repository is also discussed because of the influence of Eh on the sorption behaviour of some nuclides.

1.1 Objectives

The work described here was undertaken in support of the Wellenberg site safety analysis. Modelling of the Wellenberg near-field chemistry was required to describe:

- composition of the pore solution;
- composition of the cement phase;

- porosity of the cement (or concrete) system;
- redox conditions of the pore solution;
- reaction of the cement additives

as a function of both time after repository closure and, in a simplified way, location in the repository. Discussion of the reaction of the inorganic waste and degradation products of the organic waste materials is included because of possible influence on the degradation of cement.

1.2 Repository conditions

1.2.1 Overview

The planned Wellenberg repository comprises a series of horizontal disposal caverns linked via a connecting tunnel to the waste reception facility and entrance zone. The planned caverns are 14m wide and 18m high. The volume of waste, around 100000m^3, requires 1850m of disposal cavern in total, which corresponds to at least 6 caverns between 200 and 300m in length. The facility will be excavated in marl host rock beneath 500-700m of rock overburden. The caverns are lined with concrete and backfilled, after stacking of the waste containers, with gas permeable concrete (NAGRA 1993b).

Two water compositions have been recovered from boreholes in the Wellenberg area: a shallower, dilute $NaHCO_3$ water and a deeper NaCl brine (NAGRA 1993c, tables 5.1.5 and 5.1.6). Both water compositions have been used in the modelling to encompass the possible range of effects from groundwater interaction.

1.2.2 Cavern segments

The SMA repository is planned to contain waste from the operation and decommissioning of nuclear power plants, from the reprocessing of spent fuel and also waste from medicine, industry and research. These different waste types are consolidated with different cements (see section 4.1) in various shapes of concrete containers. Depending on the included waste types and their concrete containers, four different cavern segments are distinguished, referred to as *cavern types*.

Cavern type 1 contains operational waste (BA), reactor waste (RA) and waste from medicine, industry and research (MIF). These wastes are predominantly in 200 litre drums which will be packed 9 or 36 to a large concrete container with the remaining space filled by gas-permeable backfill concrete;

Cavern type 2 contains decommissioning waste (SA);

Cavern type 3 contains reprocessing waste from BNFL (WA-BNF-5);

Cavern type 4 contains reprocessing waste from Cogéma (WA-COG-5).

1.2.3 Waste groups

The SMA waste types contain different amounts of materials which could influence the degradation of cement and the extent of radionuclide sorption on cement. To ensure best possible retardation of nuclides, waste types with large amounts of possible sorption-reducing material are separated from waste types with none. This is done by assembling the waste in four different groups: SMA-1, SMA-2, SMA-3 and SMA-4 (the waste type and cavern type allocation to each group is given in Appendix A). These waste groups and, thus, their domains within the repository, may show different near-field chemistry and sorption behaviour because of differences in the included waste.

1.2.4 Hydrogeology

The average groundwater flow per unit area is between $4 \cdot 10^{-11}$ m^3/m^2s and $4 \cdot 10^{-13}$ m^3/m^2s (NAGRA 1993c, table 5.1.7), a value of $4 \cdot 10^{-12}$ m^3/m^2s is used for the base case; the direction of flow with respect to cavern orientation is not certain and the two extreme cases of parallel and perpendicular flow are considered for modelling purposes.

1.3 Near-field chemistry modelling strategy

1.3.1 General points

The cement degradation model of BERNER (1990) describes the incongruent dissolution of the calcium-silicate-hydrate (CSH) gel phase of the cement. The model was extended with the addition of aluminium-bearing phases hydrogarnet ($Ca_3Al_2(OH)_{12}$) and ettringite ($Ca_6Al_2(SO_4)_3(OH)_{12} \cdot 26H_2O$) to better describe the cement composition. Magnesium, in the form of brucite ($Mg(OH)_2$), was included in the original model but an attempt was made to replace it with hydrotalcite ($Mg_4Al_2(OH)_{14} \cdot 3H_2O$), a more important host for magnesium (ATKINS et al.1992).

The cement degradation model is incorporated in the FORTRAN code DISSOLVE (see BERNER 1990 and 1987). This simulates the results of a batch experiment in which 1kg of hydrated cement reacts to equilibrium with successive aliquots of groundwater. The volume of water in each cycle corresponds to the pore volume of the 1kg sample and changes throughout the experiment as cement phases dissolve and secondary minerals, e.g. calcite, are precipitated. The pore water composition, pH, porosity and remaining solid phase composition at selected cycles are included in the output from the program. DISSOLVE is used in conjunction with the Nagra thermochemical database (PEARSON & BERNER 1991; PEARSON et al. 1992). All the modelling described here was for 25°C, the expected repository temperature, and pressure of 1 bar. No attempt was made to modify the thermodynamic data for calculations at the higher hydrostatic and possibly lithostatic pressure which might be expected in the repository. However, it is expected that pressure corrections would have little effect on the overall results as the pressure difference and molar volume of reaction are relatively small.

The approach taken throughout is essentially pragmatic; for example, where there is uncertainty about a process or insufficient data etc. to calculate the effect of that process, the result for the worst possible case is estimated so that this can be used to establish the maximum effect of the process. From this it should then be clear whether further work is needed to better evaluate a process that could potentially have a large influence on the repository system, or whether the effort could be better utilised elsewhere as even the worst possible effect is not significant.

1.3.2 Undisturbed concrete and steel system

The degradation of individual cement types was modelled using the two Wellenberg groundwater types. The model system consisted only of the hydrated cement, porosity which controlled the amount of groundwater present in each cycle, and the groundwater itself. The quartz aggregate in concrete was considered inert, i.e. only the behaviour of the cement component of the concrete was considered, but blending agents (e.g. pulverised fuel ash, PFA, or trass) were included in the cement composition as they are considered reactive. No other influences were considered, for example, reaction between steel and cement, or between waste and cement.

The degradation of averaged concrete compositions, reflecting the proportions of different cements used in each cavern type, was modelled in the same way. These averaged concrete compositions clearly do not represent accurately the concrete within the repository sections as no account is taken of the heterogeneity caused by distribution of the different concrete types. The purpose of modelling with averaged compositions was to give an indication of the effect of a mixed concrete type on the duration of the high pH porewaters. Future model developments will aim to give a better representation of the spatial variations in the concrete of repository sections.

For the averaged cavern type concretes, and also the gas permeable backfill concrete, the changing porosity of the system was also determined.

1.3.3 Effect of disturbing factors

As the cement and concrete in the repository may be affected by the presence of other components of the repository, the modelling was extended to include some of these possibilities. Of particular concern are reactions between the cement and degradation products of the organic materials. Besides the large volumes of organic waste in the repository, some common types of cement additives are organic polymers. Uncertainty about the longterm fate of organics in the repository means that modelling their influence is difficult. However, an attempt has been made to assess the possible scale of their influence on the degradation of the cement.

Various metals (e.g. decommissioning waste) form the largest part of the inorganic waste materials. Of these, Fe in the form of steel, Al and Zn are important because of their influence on the Eh of the repository system. The influence of other inorganic waste components is likely to be small because they are present in relatively small amounts. Also, some waste, such as glass and ash, are composed of oxides, predominantly silica and alumina, which will not dissolve quickly enough under the expected repository conditions to significantly affect the cement-buffered porewater. The ash composition is not precisely known and its large carbon content may include partially oxidised organics. The effect of this is clearly dependent on its composition.

2 MODIFICATIONS TO THE CEMENT DEGRADATION MODEL

The cement degradation model of BERNER (1990) describes the chemistry of cement in terms of only the CSH gel phase, the alkali hydroxides, KOH and NaOH, and brucite ($Mg(OH)_2$). To allow the model to more completely describe cement degradation two changes were made:

- Two solid phases were added to incorporate aluminium (hydrogarnet) and sulphate (ettringite) in the cement model;
- The model for alkali hydroxide dissolution was improved to better simulate experimental data.

An attempt was also made to replace the Mg host mineral, brucite, with hydrotalcite ($Mg_4Al_2(OH)_{14}{\cdot}3H_2O$ or M_4AH_{10}[1]) to give a more realistic phase assemblage. Unfortunately, it appears from the experimental data of ATKINS et al. (1992) that this phase dissolves incongruently, at least at high pH. Consequently, a single $LogK_{sp}$ is not adequate to describe its behaviour over the pH range of interest. The possibility of describing the incongruent dissolution in terms of two independent components, $Al(OH)_3$ and $Mg(OH)_2$, with separate solubility constants was not implemented due to time constraints on the project and the significant amount of reprogramming of DISSOLVE which would have been necessary with this option. Instead, it was assumed that Al in solution would be dominated by the dissolution of hydrogarnet and ettringite, and that a single solubility product for $Mg(OH)_2$ could be used (see Appendix C). This produced a reasonable simulation of Mg concentration obtained in compatibility experiments[2] (ATKINS et al. 1992).

---

[1] Cement notation is used throughout: C denotes CaO; S: SiO_2; H: H_2O; A: Al_2O_3; M: MgO; $\overline{S}$: SO_3 etc. Hence $Mg(OH)_2$ becomes MH and hydrogarnet $Ca_3Al_2(OH)_{12}$ becomes C_3AH_6

[2] Compatability experiments test the stability of a mineral assemblage, under specific conditions, relative to other possible assemblages. For example, hydrotalcite and portlandite might be sealed together with a quantity of water at, say, 25°C, for a period of weeks or months until equilibrium is assumed to have been attained. On opening, the solution is analysed for Ca, Mg and Al concentrations and pH or possibly OH^- concentration, and the solids examined by SEM/TEM and XRD to detect any new phases which might have precipitated at the expense of hydrotalcite or portlandite, indicating that this was not the stable assemblage at the conditions of the experiment.

2.1 Additional cement phases

2.1.1 Hydrogarnet

The inclusion of hydrogarnet ($Ca_3Al_2(OH)_{12}$ or C_3AH_6) in the cement model allows some predictions to be made about the behaviour of aluminium in the cement-pore water system. Although hydrogarnet is not as abundant as the CSH phase in cement, it is nonetheless a significant phase constituting up to 8 wt.% of hydrated cement[3]. However, the importance of hydrogarnet to the model is in allowing a more realistic assessment of pH when the Ca/Si (C/S) ratio in the CSH phase approaches 1.0 and the pH would fall sharply in the absence of hydrogarnet.

The derivation of a solubility constant ($LogK_{sp}$) for hydrogarnet is given in detail in Appendix C. In brief, the experimental data of ATKINS et al. (1992) was used to derive a solubility constant for the reaction

$$Ca_3Al_2(OH)_{12} + 12H^+ \leftrightarrow 3Ca^{2+} + 2Al^{3+} + 12H_2O$$

$$(LogK_{sp} = 80.8)$$

and the predictions for solution compositions using this value were compared with the results from compatibility experiments by the same authors.

2.1.2 Ettringite

Ettringite ($Ca_6Al_2(SO_4)_3(OH)_{12}{\cdot}26H_2O$ or $C_6A\overline{S}_3H_{32}$) is another important minor component of hydrated cement constituting up to 10 wt. % of hydrated cement. It is the thermodynamically stable sulphate-containing phase in the hydrated cement assemblage although the monosulphato-aluminate phase ($C_4A\overline{S}H_{12}$) may also be present or replace ettringite in cement compositions low in sulphate (ATKINS et al. 1992). The dissolution of ettringite may promote the precipitation of gypsum ($CaSO_4{\cdot}2H_2O$), thus modifying the porosity of the system.

A solubility constant for ettringite was determined from the experimental data of ATKINS et al. (1992). The experimental results for this phase appear less good than for hydrogarnet, insofar as there are larger charge imbalances and greater deviations from ideal solution compositions. However, the predicted solution compositions for the compatibility experiments (ATKINS et al. 1992) compared adequately well with the experimental values (see Appendix C). For the reaction:

$$Ca_6Al_2(SO_4)_3(OH)_{12} + 12\,H^+ \leftrightarrow 6Ca^{2+} + 2Al^{3+} + 3SO_4^{2-} + 12H_2O$$

$$LogK_{sp} = 57.0.$$

---

[3] This is the Al endmember only: Fe^{3+} may substitute for Al forming an Fe-hydrogarnet. The dissolution of this phase is not yet included in the model because of uncertainty about which minerals are hosts for Fe in hydrated cement and the lack of thermodynamic data. In the method used here (BERNER 1987) to calculate cement mineralogy from the chemical composition, Fe is assigned to either hydrogarnet or Fe_2O_3.

2.2 Variation in the hydrogarnet solubility product

In the Berner cement model (BERNER 1990), the incongruently dissolving CSH phase is represented by two model phases "$Ca(OH)_2$" and "SiO_2"[(4)] which, although they have the same chemical composition as portlandite and quartz, are assigned different solubility products. These model phases do not exist in reality but are entities which can be used to describe the behaviour of the single $Ca_xSi_y(OH)_z$ phase.

Unfortunately, because of the addition of hydrogarnet to the cement model, problems arose when the concentration of Al in solution was high enough to exceed the solubility of gibbsite (AH). The hydrogarnet could then be described by the combination of the AH and the "$Ca(OH)_2$", and the hydrogarnet - CSH - AH system was found by the DISSOLVE program to contain four phases (AH, hydrogarnet, "$Ca(OH)_2$" and "SiO_2") in apparent violation of the phase rule for the Ca-Al-Si-OH system. In reality, hydrogarnet can coexist with gibbsite and the CSH phase (e.g. D'ANS & EICK 1953) but not with gibbsite and portlandite at equilibrium. However, in order for the cement degradation model to run in the DISSOLVE program, the precipitation of AH must be suppressed. This was done by linking the $LogK_{sp}$ of hydrogarnet to the solubility product of the AH and the "$Ca(OH)_2$" model phase by the relationship:

$$LogK_{sp\,(HG)} - 3LogK_{sp(\text{"}Ca(OH)_2\text{"})} > 2LogK_{sp(AH)}$$

In this way, the hydrogarnet $LogK_{sp}$ remains unchanged as long as the model $LogK_{sp(\text{"}Ca(OH)_2\text{"})}$ doesn't change, $LogK_{sp(AH)}$ being constant. However, $LogK_{sp(\text{"}Ca(OH)_2\text{"})}$ decreases as the C/S ratio of the CSH gel is reduced below 2.5 (BERNER 1990) and the hydrogarnet solubility reduced accordingly. In this way the Al concentration could be held just below the saturation limit of AH for any solution pH. When hydrogarnet has dissolved, the Al concentration is controlled by the dissolution of any remaining ettringite and the precipitation of AH is allowed.

In practice, as long as the C/S ratio of the CSH phase is well above 1.0, the hydrogarnet $LogK_{sp}$ is not changed as the change in $LogK_{sp(\text{"}Ca(OH)_2\text{"})}$ is small. As "$Ca(OH)_2$" dissolution from the CSH gel controls the pH, the small changes in $LogK_{sp(\text{"}Ca(OH)_2\text{"})}$ result in only a very slow fall in pH. Thus, hydrogarnet dissolution is slow and Al concentrations in solution remain low. However, as the C/S ratio approaches 1.0, the pH starts to fall rapidly as $LogK_{sp(\text{"}Ca(OH)_2\text{"})}$ changes quickly. At this point the hydrogarnet dissolution increases and the concentration of Al in solution rises to about 7mmol/dm^3 causing the $LogK_{sp}$ restriction to operate. The effect of this is to reduce the solubility of hydrogarnet and, therefore, to prolong its existence in the system. The number of extra cycles in which hydrogarnet is still present is large with cement compositions which contain relatively large amounts of hydrogarnet. This then has repercussions for the rate of ettringite dissolution and the amount of AH precipitated. In systems where there is initially only a small amount of hydrogarnet, most of it will have dissolved before the pH falls significantly.

Overall, the effect of this mechanism on the duration of porewater pH above 11.0 is quite small. The increased duration of hydrogarnet in the system causes the pH to

---

[4] In order to avoid confusion when referring to the model phase "$Ca(OH)_2$" or the mineral portlandite, only the latter will be abbreviated to CH and the model phase will be spelt out in full (i.e. "$Ca(OH)_2$"). Likewise, the model phase "SiO_2" will be described thus.

remain slightly higher for these extra cycles than would have been the case without the change in its $LogK_{sp}$. However, this is compensated by the reduced amount of AH which is allowed to precipitate. The AH is the last Al phase to dissolve and buffers the pH above the background (groundwater + calcite) value in the absence of hydrogarnet and ettringite. Table 1 shows the effect of the hydrogarnet $LogK_{sp}$ changes on two cement compositions compared to the results using an unmodified $LogK_{sp}$.

Backfill cement (Sulfacem, 24% porosity) Low hydrogarnet content		**Cavern Lining** (Average Swiss PC, 6.4% porosity) High hydrogarnet content	
Modified $LogK_{sp}(HG)$	Unmodified $LogK_{sp}(HG)$	Modified $LogK_{sp}(HG)$	Unmodified $LogK_{sp}(HG)$
Cycle at which hydrogarnet is all dissolved		Cycle at which hydrogarnet is all dissolved	
306	300	2202	1410
pH = 12.12	pH = 11.99	pH = 11.24	pH = 11.86
Cycle at which pH falls below 11.0		Cycle at which pH falls below 11.0	
593	591	2334	2321

Table 1: Comparison of the effect of changing hydrogarnet $LogK_{sp}$ on two cements. For each example, results are given for a calculation in which the hydrogarnet $LogK_{sp(HG)}$ was allowed to vary to stop the precipitation of AH (Modified $LogK_{sp(HG)}$) and for a calculation which was made in parts so that AH precipitation could be suppressed temporarily without changing $LogK_{sp(HG)}$.

To obtain results without the hydrogarnet $LogK_{sp}$ restriction, it is necessary to start the degradation model (DISSOLVE code) with AH precipitation completely suppressed which means that Al concentration in solution rises to unrealistic values around 25 $mmol/dm^3$ before the hydrogarnet is dissolved. The amount of AH which should have precipitated in the cycles in which the Al concentration was above about 7 $mmol/dm^3$ can be calculated. This value is then used as an input parameter for a second run of the DISSOLVE code starting at the cycle at which hydrogarnet was finally dissolved. The amounts of components remaining at this cycle, as calculated in the first run, are used as the starting input values for the second run. For the second run, AH is allowed to precipitate or the amount input to dissolve. The results in Table 1 are from the combined output of the first and second runs. Besides being a tedious method, this technique does not give an exact answer as the high Al concentrations which occur in the first run influence the system differently to lower concentrations. However, this effect is very small and it is clear that the ultimate effect of changing the hydrogarnet $LogK_{sp}$ on the prediction of the duration of the high pH porewater is also small, well within the uncertainty of the model.

2.3 Dissolution of the alkali hydroxides

The 1 wt.% of hydrated cement comprised of alkali hydroxide (KOH and NaOH) has a major influence on the pH of the cement pore water in the early stages of degradation. Unlike portlandite, the dissolution of these phases is not limited by their solubility but by their physical access to the pore water, hence, highly alkaline pore solutions can form. Early cement porewater is known to have a pH commonly in excess of 13.5 (see LEA 1970, and TAYLOR 1990).

The BERNER (1990) cement degradation model used an incremental method for alkali dissolution, whereby a small percentage, usually 5 or 10%, of the remaining alkalis in the cement are dissolved in each cycle until <0.1% of the initial amount remains which is dissolved in the next cycle. However, experimental data for cement dissolution show that the rate of alkali loss is much greater than this, at least initially. From the experimental data, the rate of loss was found to be very close to 45% of remaining alkalis per cycle, at least for the first 8 cycles, after which the concentrations of K and Na remained nearly constant in the pore water. There is not a great difference between the dissolution rates for KOH and NaOH; only about 1% more KOH than NaOH is dissolved per cycle. The cement used in these experiments has a high water to cement ratio resulting in a high porosity (65%). However, the flow rate was also high and one cycle of pore water exchange took only 80 hours. These two effects should counteract each other to some extent. When a rate of 45% per cycle was used for the alkali dissolution (using the same value for NaOH and KOH), the resulting pH for a cement of normal porosity (water/cement ratio of 0.4 to 0.5) and low to moderate alkali content (<1wt.% Na_2O + K_2O) was around 13.5 for the first cycle. This is the highest pH that can be used in calculations in the current version of DISSOLVE because of problems with high ionic strength solutions for which there are no appropriate algorithms in the program. Thus, in practical terms, the value for the rate of alkali dissolution derived from the experimental data can be used for average cement types to give a prediction for the initial pore water pH in good agreement with observations (e.g. TAYLOR 1990).

The problems arise in the treatment of high alkali cements or cements with low porosity. In these cases, dissolving 45% of the alkalis in the first cycle can result in solution ionic strengths over 1.0 M which are outside the limit of what DISSOLVE can reliably model. To stay within the limits of DISSOLVE, the amount of alkalis dissolving in the first cycle has been limited so that their maximum concentration in the pore solution is 0.5 moles/dm^3, producing a maximum pH of 13.5. This extends by one or two cycles the lifetime of the alkalis in the cement. For the normal cements (porosity = 18%, alkalis = 1%), less than 1% of the initial alkalis remain after 8 cycles and <0.1% after 12 cycles. For a lower porosity, high alkali cement (porosity = 16%, alkalis =1.27%) these levels are at 10 and 15 cycles, respectively. This restriction may not be an entirely artificial effect as, in a low porosity cement, the pore water will not be able to access as much of the alkalis as in a cement with higher porosity. Therefore, the dissolution rate of the alkalis could be lower in lower porosity cements. On a practical note, the pH falls to 12.55 after 5 cycles for both high and normal alkali cements; at this point the dissolution of "$Ca(OH)_2$" from the CSH is the dominant factor controlling the pH.

3 GROUNDWATERS

The degradation of the individual and averaged cement compositions was modelled in two different groundwaters:

- the Wellenberg $NaHCO_3$ type (NAGRA 1993c, table 5.1.5)
- the Wellenberg NaCl type (NAGRA 1993c, table 5.1.6)

The compositions used in DISSOLVE are slightly different from those given in that report (NAGRA 1993c). The differences result mainly from reduction of the total number of components used in the degradation modelling. It was expected that the presence of components such as B, Li, As, Zn, Cd, Pb etc. would have no effect on the system so their concentration was added to that of abundant but unimportant ions. For example, Li was added to Na, B and As to Cl, so that the charge balance and ionic strength of the solution were maintained while simplifying the speciation calculation. Also, for the NaCl water, the concentration of Ca^{2+} and HCO_3^- were both reduced by 10% to make the groundwater slightly undersaturated with respect to calcite. The composition of the two reference waters as used in the modelling is given in Table 2.

Table 2: Composition of the Wellenberg Reference waters as used in this study

Components	Wellenberg $NaHCO_3$ water	Wellenberg NaCl water
Ca_{total}	$5.72 \cdot 10^{-5}$ M	$3.98 \cdot 10^{-3}$ M
Mg_{total}	$3.28 \cdot 10^{-5}$ M	$3.38 \cdot 10^{-3}$ M
Sr_{total}	$5.71 \cdot 10^{-6}$ M	$7.04 \cdot 10^{-4}$ M
K^+	$5.11 \cdot 10^{-5}$ M	$7.10 \cdot 10^{-4}$ M
Na^+	$1.75 \cdot 10^{-2}$ M	$4.61 \cdot 10^{-1}$ M
Fe^{3+}	$1.53 \cdot 10^{-10}$ M	$1.39 \cdot 10^{-12}$ M
Fe^{2+}	$5.37 \cdot 10^{-7}$ M	$9.20 \cdot 10^{-7}$ M
Mn_{total}	$3.64 \cdot 10^{-7}$M	$1.12 \cdot 10^{-5}$ M
Al_{total}	$3.71 \cdot 10^{-7}$ M	-
Total carbonate	$1.61 \cdot 10^{-2}$ M	$3.39 \cdot 10^{-3}$ M
Total sulphate	$1.15 \cdot 10^{-4}$ M	$1.07 \cdot 10^{-5}$ M
Cl^-	$2.96 \cdot 10^{-4}$ M	$4.72 \cdot 10^{-1}$ M
F^-	$9.47 \cdot 10^{-4}$ M	$9.72 \cdot 10^{-7}$ M
Br^-	-	$2.68 \cdot 10^{-3}$ M
I^-	-	$5.20 \cdot 10^{-4}$ M
NH_3	$3.88 \cdot 10^{-5}$ M	$5.53 \cdot 10^{-4}$ M
Total phosphate	$6.46 \cdot 10^{-6}$ M	$1.34 \cdot 10^{-5}$ M
Total silicate	$1.74 \cdot 10^{-4}$ M	$2.06 \cdot 10^{-4}$ M
NO_3^-	$1.61 \cdot 10^{-6}$ M	$1.66 \cdot 10^{-6}$ M
pH	8.3	7.5
Eh	-125 mV	-125 mV
Ionic Strength	$1.80 \cdot 10^{-2}$ M	$4.86 \cdot 10^{-1}$ M
Log P_{CO2}	-2.3	-2.3
Temperature	25°C	25°C
Pressure	1 bar	1 bar

4 MODELLING DEGRADATION OF SINGLE CEMENT COMPOSITIONS

4.1 Cement types in the repository

The SMA repository is constructed from the six different types of cement specified in Table 3 (present stage of planning). Their chemical compositions and porosities are given in Table 4. From the chemical composition, the hydrated mineralogy of each cement (Table 5) was calculated according to BERNER (1987). Two options exist for the backfill concrete: the first option, with the composition given in Table 4, has been investigated by JACOBS et al. (1994). The second option differs from the first by the use of a reactive aggregate, ideally crushed hydrated cement, in place of quartz sand. This second option is not explicitly considered here as its degradation behaviour will be the same as, but slower than, that of the first option.

The "free oxides"[1] (Table 4) are contributed by the blending agents, i.e. trass and pulverised fuel ash (PFA), in the blended cements. Where the amount of blending agent is small relative to the amount of cement, the blending agent is assumed to react fully with the cement and to be incorporated into the cement mineralogy (e.g. HTS + trass). When the proportion of blending agent is larger, such as in the OPC + 75% PFA in cavern Type 3 waste cement, to assume that all of it reacts produces a chemical composition that can no longer be described in terms of cement mineralogy because of the high Al_2O_3 and SiO_2 and low CaO. However, to consider that it is inert like the quartz aggregate and that none of it reacts is also clearly unreasonable when it constitutes 75 weight percent of the dry cement. It is possible to combine part of the blending agent and ignore the rest but an arbitrary decision has to be made about the proportion, so that nearly any cement composition can be produced. This is obviously not desirable for modelling of the behaviour of a specific cement composition. Because of these difficulties, no mineralogical composition was calculated for the cavern type 3 blended cement.

4.2 Porosity

Differences between the concrete porosity (Table 4) and the cement minimum porosity (Table 5) are caused by the presence of the aggregate. The **cement minimum porosity** is the porosity of the cement without any aggregate and is the volume occupied by mixing water which is not used in the hydration reactions. It does not include any estimate of the effect of entrained air. The **concrete porosity** is calculated from the density of the aggregate (i.e. quartz sand at 2650 kg/m^3) plus the hydrated cement when the masses of cement, aggregate and water per unit volume are known. The porosity is the volume left unfilled by either the cement or aggregate.

With the exception of the backfill cement, the degradation of the other cements was modelled using the minimum porosity. For the backfill cement, it was of particular

---

[1] Except in the case of silica fume, the blending agents do not contribute actual free oxides but predominantly silicate minerals. These components are termed "free oxides" to distinguish them from oxides bound in the cement clinker.

	Waste	Container Infill	Container Walls	Cavern Backfill	Cavern Lining
Cavern Type 1	11	16	19	26	28
Cavern Type 2	32		10	30	28
Cavern Type 3	24			48	28
Cavern Type 4	16			56	28

Table 3a: Volume percentages of the different cement types used in the SMA repository (derived from NAGRA 1993a)

	Waste	Container Infill	Container Walls	Cavern Backfill	Cavern Lining
Cavern Type 1	HTS/trass	SulfacemH	SulfacemN	SulfacemH	APC
Cavern Type 2	OPC		OPC		
Cavern Type 3	OPC/PFA				
Cavern Type 4	OPC				

Table 3b: Types of cement used in the SMA repository

APC	Average Swiss Portland Cement
SulfacemH	Sulphate-resistant cement (High Porosity - gas permeable)
SulfacemN	Sulphate-resistant cement (Normal Porosity)
HTS/trass	Portland cement (**H**aute **T**eneur en **S**ilice) + trass blending agent
OPC	Ordinary Portland Cement
OPC/PFA	OPC + Pulverised Fuel Ash

Table 3c: Abbreviations for the different cement types

interest to see the influence of the large concrete porosity on the rate of degradation of this cement. (Note: cavern type 1 walls cement has the same composition as the backfill cement but normal (i.e. minimum) porosity.) For this reason the concrete porosity of 24% was converted into a model porosity for input to the DISSOLVE program.

The **model porosity** is based on the actual amount of water in a volume of the concrete compared to the amount of cement in the same volume of concrete. For example, a concrete composed of 1.3 kg of hydrated cement and 4.5 kg of aggregate with an overall (concrete) porosity of 9% has a model porosity of 27% because:

The volume of the 5.8 kg of concrete = $2.24dm^3$
The volume of the porosity in $2.24dm^3$ = $0.202dm^3$ (9% of $2.24dm^3$)
The volume of 1.3kg of hydrated cement = $0.546dm^3$

Oxides (wt. %)	**SulfacemH** cavern backfill	**APC** cavern lining	**SulfacemN** cavern type 1 walls	**HTS/Trass** cavern type 1 waste	**OPC** cavern type 2/4	**OPC/PFA** cavern type 3 waste
Fe_2O_3	7.25	2.9	7.25	1.23	3.2	0.8
Al_2O_3	4.00	5.10	4.00	2.13	4.50	1.12
SiO_2	20.50	21.30	20.50	19.77	23.00	5.74
CaO	62.00	63.80	62.00	55.86	64.00	15.97
SO_3	2.75	2.80	2.75	1.76	3.00	1.20
Free Fe_2O_3	-	-	-	1.15	-	7.73
Free Al_2O_3	-	-	-	3.61	-	19.51
Free SiO_2	-	-	-	10.30	-	40.52
Free CaO	-	-	-	0.97	-	2.62
K_2O	1.00	1.04	1.00	1.14	0.6	1.88
Na_2O	0.10	0.23	0.10	0.38	0.60	1.28
MgO	1.20	2.10	1.20	0.81	0.80	1.40
TiO_2	-	0.27	-	-	0.30	0.08
Other	1.20	0.56	1.20	0.50	-	-
w/c	0.4	0.43	0.43	0.44	0.5	0.44
Agg/c	5.33	5.57	5.57	-	4.53	-
Concrete ρ	1918	2450	2450	2025	2400	1640
Concrete ϕ	24(1)	6.4	6.8	25.5	9.2	<45(2)

w/c : water to cement ratio (kg/kg)
Agg/c : aggregate to cement ratio (kg/kg)
Concrete ρ : concrete density (kg/m^3)
Concrete ϕ : concrete porosity (%)

(1) This is the given porosity based on the porosity of the aggregate minus the volume of the cement. However, the cement also contains a further 3%, possibly micro-, porosity from the unused mixing water. The value used in the modelling is the 24% of measured macroporosity (JACOBS et al. 1994).

(2) Although the effect of the PFA blending agent is to produce a low density, high porosity concrete, a high proportion of the porosity is not connected and the resultant permeability is low (BERRY et al. 1989)

Table 4: Chemical compositions of the different types of cement used in the SMA repository and their associated concretes.

$$\text{Model porosity} = \frac{\text{total volume of porosity}}{\text{total volume of the cement system (i.e. without aggregate)}}$$

$$= \frac{\text{volume of the concrete porosity}}{\text{volume of the cement + volume of the concrete porosity}} = 27\%$$

The model porosity is required because the cement is dissolved by all the water in a volume of concrete not just the water in the porosity associated with cement which constitutes only about 20% of the concrete volume. For some cement types the model porosity is not substantially different from the minimum porosity (Table 5) but for the backfill cement the model porosity is 53%, some 3 times larger than the cement minimum porosity. Where there is no aggregate (e.g. cavern type 1 waste: HTS + trass) the minimum porosity and the model porosity are the same.

Mineral	SulfacemH cavern backfill	APC cavern lining	SulfacemN cavern type 1 walls	HTS/Trass cavern type 1 waste	OPC cavern type 2/4	OPC/PFA cavern type 3 waste*
C_3FH_6	0.324	0.127	0.317	0.078	0.133	
C_3AH_6	0.145	0.178	0.142	0.307	0.179	
$C_{1.8}SH_{1.8}$	2.437	2.479	2.386	-	2.552	
$C_{1.61}SH_{1.61}$	-	-	-	3.471	-	
$C_6A_3\bar{s}H_{32}$	0.081	0.082	0.080	0.051	0.083	
$Ca(OH)_2$	1.611	2.092	1.578	-	1.576	
M_4AH_{10}	0.054	0.091	0.052	0.035	0.033	
KOH	0.151	0.155	0.148	0.168	0.085	
NaOH	0.023	0.052	0.022	0.085	0.129	
Free Fe_2O_3	-	-	-	0.025	-	
Free TiO_2	-	0.024	-	-	-	
Density kg/m^3 (1)	2126	2063	2084	2025	1965	1640
Minimum ϕ	16.0%	17.4%	18.4%	25.5%	26.0%	-
Model $\phi^{(2)}$	53.0%	24.6%	26.1%	25.5%	27.0%	-

(1) density calculated from the mass/volume of the hydrated minerals + excess mixing water.

(2) hypothetical cement porosity which gives the correct ratio of pore water to hydrated cement for the corresponding concrete composition, see text for details of the calculation.

Table 5: Mineralogical compositions, in moles per kg of hydrated cement, density and porosities of the six hydrated cement types used in the SMA repository.

It should be noted that, in this study, no account is taken of possible differences in permeability between the different concretes. This could be of some importance to the concretes containing blending agents (cavern types 1 and 3 wastes) which have high porosities which, in turn, have a detrimental effect on the lifetime of the high pH pore water. In reality, these concretes are likely to have a much smaller effective porosity (i.e. connected porosity), as indicated by their relatively poor permeability (see for example, BERRY et al. 1989). However, as the effective porosity was not known, the total porosity was used in calculations yielding a conservative, or worst case, result.

4.3 Results of the degradation model

The results of the degradation modelling for the cavern lining cement (in Wellenberg $NaHCO_3$ water) in terms of the changing pore fluid composition with increasing cycles of pore water exchange are given in Figure 1. A summary of the pH evolution for each of the individual cement compositions is presented in Figure 2. Full results for all the individual cement compositions are given in Appendix B. The approximate cycle numbers at which the pH falls below 11.0 and to background levels (i.e. there is no

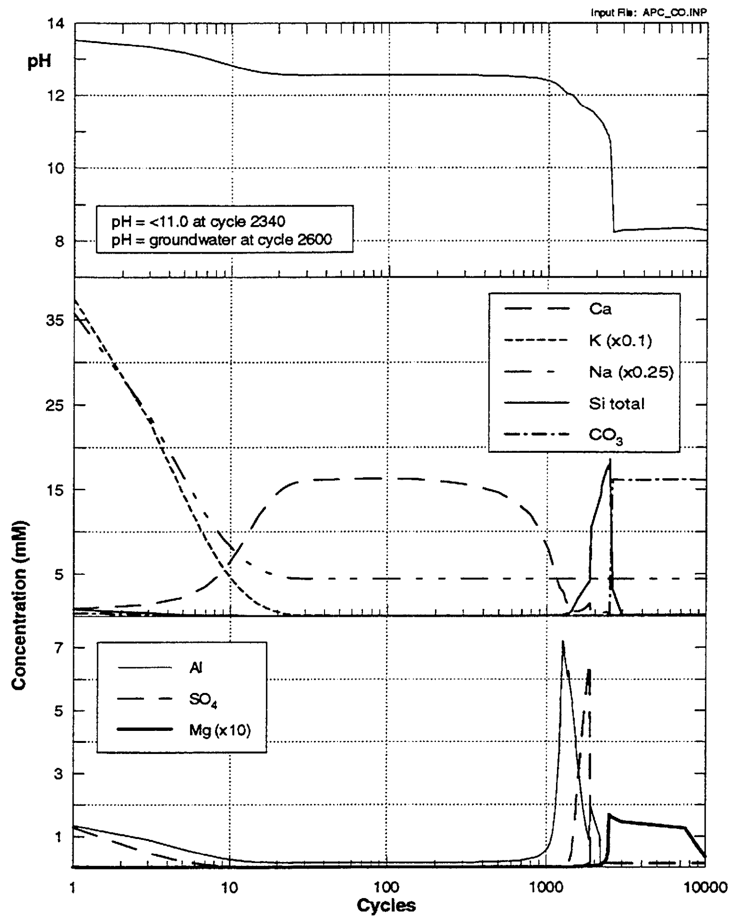

Figure 1: Results of the cement degradation modelling for cavern lining cement (average Swiss Portland cement) in Wellenberg $NaHCO_3$ water

longer any contribution from the cement) are also given in Table 6. Table 7 gives the porewater chemistry at selected cycles for cavern lining cement.

As described in Berner (1990), the degradation generally shows 3 stages:

- In the first stage, the pH is dominated by the dissolution of the alkali hydroxides resulting in an initial value around 13.5. With the new higher rate for their dissolution this stage becomes much shorter than in the previous model, lasting only about 10 cycles. The Ca concentration rises sharply to its maximum value as the K and Na concentrations and pH fall. Once the pH has fallen to about 12.5, it is controlled by the dissolution of "$Ca(OH)_2$" from the CSH gel. The ionic strength in the first stage is higher than in later cycles due to the high alkalis. This slightly enhances the dissolution of the other phases so Al, Mg and SO_4 in solution are initially higher than through the rest of the high pH plateau (stage 2).
- In the second stage, the pH is dominated by the "$Ca(OH)_2$" in the CSH gel. The pH and Ca concentration in the pore fluid fall steadily throughout this stage as the C/S ratio in the CSH is reduced by the incongruent dissolution. Around pH 12.0, as the C/S ratio approaches 1.0, the pH begins to fall more rapidly and the

dissolution of the hydrogarnet increases resulting in a rapid rise in the Al concentration. This marks the end of the second stage and occurs between about 200 cycles (backfill cement) and 1000 cycles (cavern lining cement in $NaHCO_3$ groundwater).

- The third stage is the most complicated as the pH is no longer dominated by the CSH gel but by the Al and Mg minerals. First dissolution of hydrogarnet, then ettringite and any secondary (precipitated) gibbsite and finally hydrotalcite are the dominant reactions. The overlapping dissolution of the aluminium phases produces a composite peak for Al concentration in solution in which the first, and highest, contribution is from hydrogarnet dissolution, then there is often a second peak or a shoulder on the first from ettringite dissolution and a third peak or long tail to the hydrogarnet peak due to the gibbsite. Once the CSH phase C/S ratio is reduced to close to zero, the remaining SiO_2 dissolves very quickly to give a sharp peak in the Si concentration which drops as the SiO_2 in the system is exhausted. In this final stage the solution chemistry changes rapidly and drastically, reflecting the waning control of the CSH phase and the effect of the other cement phases.

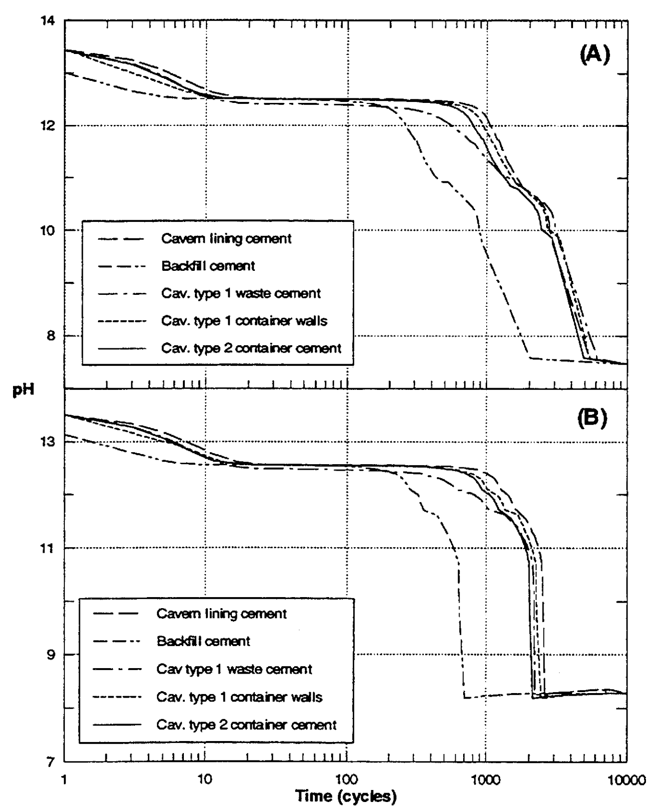

Figure 2: Evolution of cement pore fluid pH with increasing cycles of pore water exchange during degradation for the five cement types used in the SMA repository in:
(A) Wellenberg NaCl water and (B) Wellenberg $NaHCO_3$ water.

The influence of the trass blending material in the cavern type 1 waste cement can be seen in the slightly lower value of the 'pH plateau' (Fig. 2) and in the earlier high Al concentrations than with other cement types (see also Figs B-1 to B-10). However, the overall duration of the high pH pore fluid is not significantly affected compared to the other cement. In general, with the exception of the backfill cement, the pore water pH drops below 11.0 after about 2000 cycles in $NaHCO_3$ water and about 1400 cycles in NaCl water. The cavern lining cement is the most long-lived mainly due to its low porosity. For the backfill cement, modelled with a large pore water volume equivalent to the concrete porosity of 24%, the high pH conditions are much shorter lived, lasting only around 590 and 430 cycles in the $NaHCO_3$ and NaCl groundwaters, respectively.

The solution composition at any individual cycle is only semi-quantitative, depending on the quality of the data for the phases etc. in the system, but the overall pattern of the evolution of the system is much more reliable. Certainly, the comparisons from one cement type to another, or between one groundwater and the other, are robust since the uncertainties are the same for each case.

As previously shown (BERNER 1990), the groundwater is commonly more important in determining the behaviour of cements than the relatively small differences in their chemical compositions. The differences in results for the $NaHCO_3$ and NaCl waters reflect the large difference in ionic strength between them. The high ionic strength of the NaCl brine causes enhanced dissolution so that the maximum Ca in solution is around 35 mmol/dm^3 compared to around 15 mmol/dm^3 in the $NaHCO_3$ water (Table 7).

Table 6: Summary of the high pH duration for the different cement types in A) Wellenberg $NaHCO_3$ water and B) Wellenberg NaCl water.

(A)	Waste	Container Infill	Container Walls	Cavern Backfill	Cavern Lining
Cavern Type 1	1970/2200	590/730	2100/2400	590/730	2340/2600
Cavern Type 2	1890/2100		1890/2100	590/730	2340/2600
Cavern Type 3	n.d.			590/730	2340/2600
Cavern Type 4	1890/2100			590/730	2340/2600

first no. /second no. : first = cycles above pH 11.0; second = cycles above groundwater pH.
n.d.: not done.

(B)	Waste	Container Infill	Container Walls	Cavern Backfill	Cavern Lining
Cavern Type 1	1300/6100	430/2000	1460/5400	430/2000	1600/5400
Cavern Type 2	1300/4900		1300/4900	430/2000	1600/5400
Cavern Type 3	n.d.			430/2000	1600/5400
Cavern Type 4	1300/4900			430/2000	1600/5400

Wellenberg $NaHCO_3$ Water							
(mmol/dm^3)	**Cycle 1**	**7**	**73**	**499**	**1097**	**1589**	**2495**
pH	13.51	13.01	12.56	12.53	12.34	11.74	10.46
Ca_{total}	0.816	3.51	16.3	14.6	5.84	0.532	0.063
Mg	$1.1 \cdot 10^{-5}$	$3.4 \cdot 10^{-5}$	$9.7 \cdot 10^{-5}$	$1.0 \cdot 10^{-4}$	$1.6 \cdot 10^{-4}$	$1.0 \cdot 10^{-3}$	0.167
Al	1.34	0.400	0.130	0.164	1.09	3.1	$3.7.10^{-4}$
K	370	91.2	0.051	0.051	0.051	0.051	0.051
Na	143	48.1	17.5	17.5	17.5	17.5	17.5
$SiO_{4\ total}$	0.767	0.092	0.017	0.019	0.038	2.19	18.5
$CO_{3\ total}$	0.328	0.260	$7.2 \cdot 10^{-3}$	$7.3 \cdot 10^{-3}$	$8.7 \cdot 10^{-3}$	0.035	0.316
$SO_{4\ total}$	1.27	0.074	$7.6 \cdot 10^{-3}$	$7.9 \cdot 10^{-3}$	0.012	2.97	0.115
C/S	2.64	2.64	2.57	2.01	1.20	0.90	0.0
Wellenberg NaCl Water							
(mmol/dm^3)	**Cycle 1**	**7**	**71**	**515**	**1095**	**1571**	**2785**
pH	13.44	12.86	12.50	12.46	11.91	11.07	10.03
Ca_{total}	1.01	8.01	35.1	32.3	16.0	10.5	5.71
Mg	$1.3 \cdot 10^{-5}$	$5.5 \cdot 10^{-5}$	$1.4 \cdot 10^{-4}$	$1.6 \cdot 10^{-4}$	$8.7 \cdot 10^{-4}$	0.025	2.53
Al	1.14	0.304	0.132	0.179	5.34	0.817	0.075
K	375	92.0	0.71	0.71	0.71	0.71	0.71
Na	587	492	461	461	461	461	461
$SiO_{4\ total}$	0.391	0.045	0.014	0.016	0.081	1.46	5.94
$CO_{3\ total}$	0.501	0.039	0.012	0.012	0.018	0.024	0.047
$SO_{4\ total}$	1.16	0.067	0.013	0.014	0.024	2.39	0.011
C/S	2.64	2.64	2.57	1.91	1.05	0.846	0.10

Table 7: Pore water chemistry at representative cycles for Cavern Lining Cement (averaged Swiss Portland cement)

5 MODELLING OF AVERAGED CAVERN TYPE CEMENTS

For each cavern type, an averaged concrete composition was calculated based on the proportions of the different constituent concretes given in Table 3. From knowledge of the individual concrete densities and porosities it is possible to calculate these parameters for the averaged cement also. The averaged concrete and cement compositions for the four cavern types are given in Table 8 and their calculated mineralogies in Table 9.

Averaged cement/concrete compositions for Cavern types 1, 2 and 4 fall within the range of normal cements. Cavern type 3, however, is substantially different in its composition because of the presence of the large proportion of PFA used in the waste matrix cement. This results in a cement formulation with a very low C/S ratio and no excess portlandite. Although the waste matrix cement constitutes only 10 wt.% of the averaged cement, the very low CaO content and high SiO_2, Al_2O_3 and MgO contents have a great effect on the overall composition. As a consequence, the average cement cannot be modelled in terms of normal cement mineralogy if all of the SiO_2 and Fe_2O_3 from the PFA are incorporated into the cement minerals. Hence, a completely arbitrary decision was made to include the CaO, Al_2O_3 and 20% SiO_2 in the mineralogical composition. Twenty percent SiO_2 is close to the limit of what can be incorporated into the cement and still have a composition which can be modelled. The Fe_2O_3 and the rest of the SiO_2 were excluded and considered inert like the normal quartz aggregate. (In the DISSOLVE code the fate of the unreacted free constituents and the quartz aggregate is not considered.) This allowed the input of the cavern type 3 averaged cement into the DISSOLVE program. However, the still marginal composition of the cement means that the model was "stretched to fit" it and the

Table 8: Oxide compositions of the averaged cement and concrete for the 4 cavern types

Oxides (wt. %)	**Cavern Type 1** Cement	Concrete	**Cavern Type 2** Cement	Concrete	**Cavern Type 3** Cement	Concrete	**Cavern Type 4** Cement	Concrete
Fe_2O_3	4.15	0.92	4.23	0.70	3.49	0.84	5.26	0.83
Al_2O_3	3.59	0.79	4.55	0.75	3.06	0.74	4.43	0.70
SiO_2	20.48	4.51	21.76	3.58	14.5	3.49	21.11	3.34
CaO	60.16	13.25	63.38	10.41	42.86	10.32	62.87	9.96
SO_3	2.42	0.53	2.87	0.47	2.11	0.51	2.80	0.44
Free Fe_2O_3	0.41	0.09	-	-	3.25	0.78	-	-
Free Al_2O_3	1.29	0.28	-	-	8.20	1.98	-	-
Free SiO_2	3.68	0.81	-	-	17.04	4.10	-	-
Free CaO	0.59	0.13	-	-	1.37	0.33	-	-
K_2O	1.06	0.23	0.85	0.14	1.38	0.33	0.96	0.15
Na_2O	0.23	0.05	0.34	0.06	0.63	0.15	0.21	0.03
MgO	1.27	0.28	1.33	0.22	1.5	0.36	1.44	0.23
Other	0.67	0.15	0.69	0.11	0.61	0.15	0.92	0.15
Aggregate	-	77.90	-	83.57	-	75.9	-	84.16
C/S	3.18	-	3.12	-	1.50	-	2.98	-
Concrete ϕ	-	16	-	13	-	21	-	17
Concrete ρ	-	2184	-	2251	-	2054	-	2127

Concrete ϕ : concrete porosity (%); Concrete ρ : concrete density (kg/m^3)

Moles / kg hydrated cement (including porewater)		Av. Cav. Type 1	Av. Cav. Type 2	Av. Cav. Type 3	Av. Cav. Type 4
C_3FH_6	Fe-hydrogarnet	0.174	0.157	0.127	0.188
C_3AH_6	Hydrogarnet	0.182	0.145	0.536	0.131
$C_{1.8}SH_{1.8}$	CSH gel	2.449	2.147	-	2.003
$C_{1.3}SH_{1.3}$	Low-Ca CSH gel	-	-	1.753	-
$C_6A\overline{S}_3H_{32}$	Ettringite	0.062	0.071	0.051	0.067
$Ca(OH)_2$	Portlandite	0.753	1.504	-	1.434
M_4AH_{10}	Hydrotalcite	0.048	0.049	0.053	0.051
KOH		0.137	0.107	0.170	0.119
NaOH		0.045	0.065	0.118	0.039
Free Fe_2O_3		-	-	0.118	-
Free TiO_2		-	-	1.289	-

Table 9: Mineralogical compositions (in moles per kg of hydrated cement - including porewater) of the 4 averaged hydrated cement compositions. Note that the composition for cavern type 3 is subject to large uncertainties.

results should be considered with this in mind. The results give some qualitative indication of the likely effect of blending agents such as PFA on the overall chemistry of the repository but should not be taken as comparable to the results for the other cement types which can be modelled with some confidence. The results of the degradation modelling in the two Wellenberg ground waters are illustrated fully for averaged cavern type 1 cement in Figures 3 and 4. Results for the three other averaged cement types are shown in Appendix B (Figs B-11 to B-16). The evolution of pH for the four averaged cement types is summarised in Fig. 5.

In Figures 3 and 4 the concomitant changes in concrete porosity are also shown. The DISSOLVE code calculates the porosity from the density and amount of minerals present in the system to update the pore volume which changes each cycle as minerals are dissolved or precipitated. The porosity calculated by the program is the model porosity but this can be simply converted back into concrete porosity because the total volume of the system is constant. Two different porosity curves are plotted in the figures (Figs 3 and 4 and B-11 to B-16): the **normal porosity** which is the percentage volume of the system occupied by water and represents an average value over the system; and the **non-precipitation (non-pptn) porosity** which is the porosity which would result if there were no secondary mineral precipitation (e.g. of calcite and fluorite). This might occur if precipitation was not uniform, i.e. it was concentrated in

Table 10: Summary of the duration of high pH in the averaged cavern type cements.

		Av. Cav. Type 1	Av. Cav. Type 2	Av. Cav. Type 3	Av. Cav. Type 4
Wellenberg	pH >11.0	1070 cycles	1000 cycles	500 cycles	760 cycles
$NaHCO_3$ water	pH > gw*	1200 cycles	1100 "	750 "	840 "
Wellenberg	pH > 11.0	800 "	740 "	300 "	590 "
NaCl water	pH > gw*	3340 "	2940 "	2500 "	2250 "

*gw: pH value of groundwater + calcite

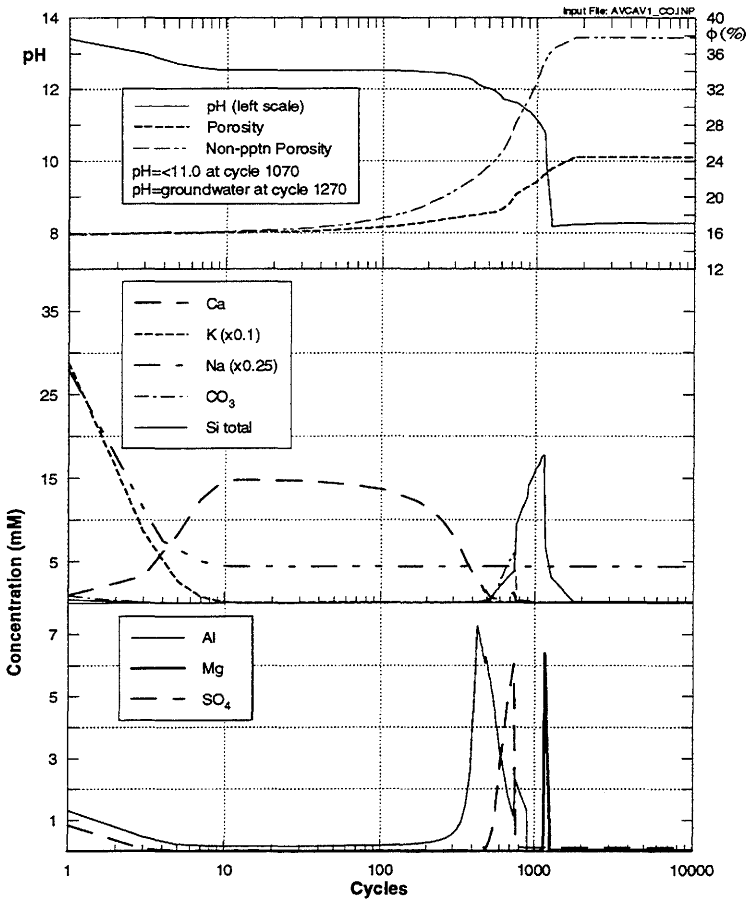

Figure 3: Results of the cement degradation modelling for averaged cavern type 1 cement in Wellenberg $NaHCO_3$ water. Non-pptn porosity is the porosity of the concrete which would arise if secondary minerals (e.g. calcite and fluorite) did not precipitate or were precipitated outside the dissolving cement volume.

some areas, resulting in variations in porosity. The non-precipitation porosity is, therefore, the maximum porosity that could develop, assuming that the quartz sand aggregate was not dissolved. The minimum porosity possible is near zero in areas of preferential mineral precipitation. The averaged cements for cavern types 1,2 and 4 are quite similar in their composition, porosity and, therefore, in their degradation behaviour. These averaged cements also behave in a very similar way to the individual cement: the 3 stages of degradation and the evolution of the porewater chemistry are the same. The duration of the high pH conditions are shorter, however, mainly due to the higher porosities used in modelling the averaged cements. In NaCl groundwater the pore-fluid pH falls below 11.0 after about 800 cycles for cavern type 1, after about 740 cycles for cavern type 2 and after about 600 cycles for cavern type 4. In the $NaHCO_3$ groundwater the durations above pH 11.0 are 1070, 1000 and 760 for the three cavern types, respectively.

Cavern type 3 averaged cement behaves differently because of the low C/S ratio of the CSH gel and the absence of free portlandite. This means that there is very little $Ca(OH)_2$, relative to the other cements, to maintain pH which drops below 11.0 after only about 500 cycles in $NaHCO_3$ water and about 300 cycles in NaCl water. That a high pH is maintained for this long is due to the larger amount of hydrogarnet in this cement. The absence of portlandite and the low C/S ratio result in substantial dissolution of the hydrogarnet and ettringite, particularly in cycles 1 to 5 of the first stage of degradation but also throughout the middle stage. Aluminium concentrations close to 1.0 mmol/dm³ occur in $NaHCO_3$ water and 0.5 mmol/dm³ in NaCl water in the middle of the second stage, compared to <0.2mmol/dm³ and 0.01 mmol/dm³ for the other averaged cements.

Table 11: pH and porewater composition (mmol/dm³) at selected cycles for two averaged cavern type cements.

Wellenberg NaCl Water								
	Averaged Cavern Type 1 Cement				**Averaged Cavern Type 3 Cement**			
Cycle No.	**11**	**323**	**599**	**1569**	**11**	**97**	**369**	**909**
pH	12.48	12.23	11.35	10.03	12.29	11.92	10.92	10.03
Ca_{total}	33.0	21.6	9.78	5.69	23.2	16.0	11.8	5.65
Mg	$1.5 \cdot 10^{-4}$	$3.1 \cdot 10^{-4}$	$7.4 \cdot 10^{-3}$	2.55	$2.6 \cdot 10^{-4}$	$8.5 \cdot 10^{-4}$	0.048	2.57
Al	0.159	0.851	1.57	0.075	0.582	5.18	0.580	0.075
K	1.42	0.71	0.71	0.71	1.42	0.71	0.71	0.71
Na	462	461	461	461	462	461	461	461
$SiO_{4\ total}$	0.015	0.033	0.652	5.93	0.028	0.080	2.03	5.91
$CO_{3\ total}$	0.012	0.015	0.025	0.047	0.014	0.018	0.022	0.048
$SO_{4\ total}$	0.014	0.019	0.738	0.011	0.018	0.024	3.85	0.011
C/S	2.08	1.22	0.924	0.10	1.28	1.05	0.793	0.099
ϕ (%)	16.2	19.4	20.5	23.7	21.7	22.3	23.5	25.3
Wellenberg $NaHCO_3$ Water								
	Averaged Cavern Type 1 Cement				**Averaged Cavern Type 3 Cement**			
Cycle No.	**11**	**339**	**590**	**1166**	**11**	**98**	**355**	**720**
pH	12.54	12.35	11.82	9.82	12.40	12.05	11.46	9.90
Ca_{total}	14.7	6.26	0.498	$9.3 \cdot 10^{-3}$	7.23	2.33	0.212	8.7e-3
Mg	$1.0 \cdot 10^{-4}$	$1.6 \cdot 10^{-4}$	$7.6 \cdot 10^{-4}$	6.37	$1.4 \cdot 10^{-4}$	$3.2 \cdot 10^{-4}$	$2.4 \cdot 10^{-3}$	4.73
Al	0.158	0.948	3.69	$3.7 \cdot 10^{-4}$	0.668	6.86	1.62	0.051
K	0.764	0.051	0.051	0.051	0.759	0.051	0.051	0.051
Na	17.7	17.5	17.5	17.5	18.0	17.5	17.5	17.5
$SiO_{4\ total}$	0.014	0.035	1.8	6.7	0.030	0.136	11.7	0.174
$CO_{3\ total}$	$7.3 \cdot 10^{-3}$	$8.5 \cdot 10^{-3}$	0.036	14.1	$8.3 \cdot 10^{-3}$	0.012	0.068	14.0
$SO_{4\ total}$	8.0e-3	0.012	2.21	0.115	0.011	0.030	0.115	0.115
C/S	2.08	1.22	0.917	0.0	1.27	1.04	0.713	0.0
ϕ (%)	16.1	17.8	18.5	23.1	21.7	21.9	24.3	28.4

ϕ : Concrete porosity

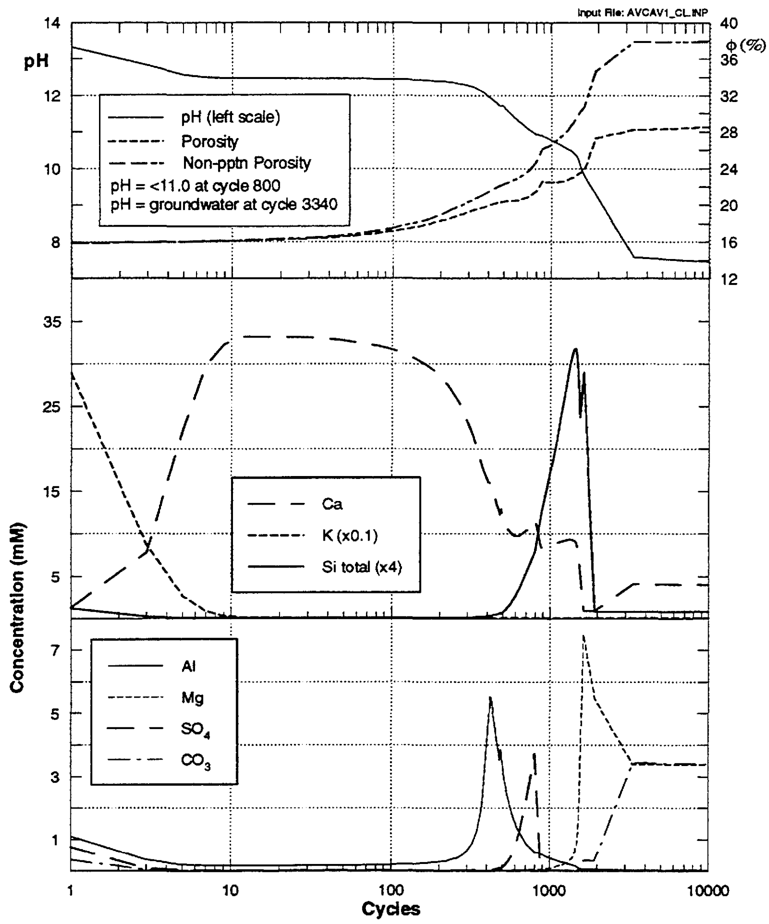

Figure 4: Results of the cement degradation modelling for averaged cavern type 1 cement in Wellenberg NaCl water.

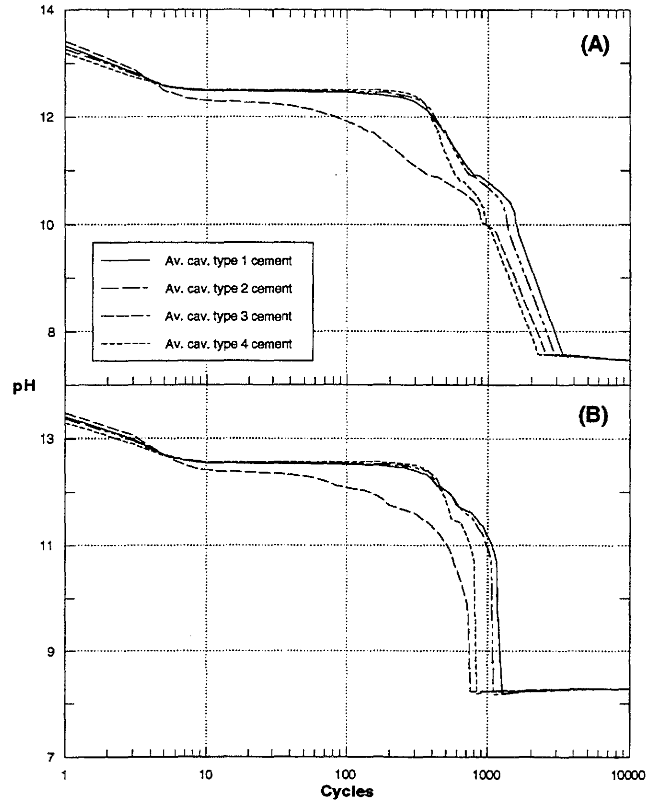

Figure 5: Evolution of cement pore fluid pH with increasing cycles of pore water exchange during degradation for the four averaged cavern type cements in: (A) Wellenberg $NaHCO_3$ water and (B) Wellenberg NaCl water.

6 LIFETIME OF THE HIGH PH CONDITIONS

Groundwater flow rate provides the link between water exchange cycles and the time in years by allowing the calculation of the time needed to exchange the porewater in a volume of concrete. The flow rate depends on two factors, the hydraulic conductivity of the geosphere, estimated at 10^{-10} to 10^{-12} ms^{-1}, and the hydraulic gradient of 0.1 to 0.4. Using the higher gradient multiplied by the hydraulic conductivity gives a range of values for the average groundwater flow rate of $4 \cdot 10^{-11}$ to $4 \cdot 10^{-13}$ ms^{-1}; a value of $4 \cdot 10^{-12}$ ms^{-1} is used for the base case calculations. The average flow rate through the repository is similar but, in detail, is affected by the hydraulic conductivity of the excavation disturbed zone and the various repository components.

For these calculations, it is assumed that flow through the repository is perpendicular to the length of the caverns. The effect of flow parallel to the cavern length is more difficult to assess due to drainage effects and is not considered here.

The duration of one porewater exchange cycle is calculated by dividing the total volume of porosity by the groundwater flux. For the both the repository component cement types and the averaged cavern type cements, the porewater exchange time is calculated for a whole cavern. However, the calculation can be simplified by considering only a representative 'tube', with a cross-sectional area of $1m^2$, across the diameter of the cavern (i.e. parallel to the direction of groundwater flow) because the water flux is given in units of cubic metres per square metre per second. Hence, taking a water flux of $4 \cdot 10^{-11}$ ms^{-1} through the repository, a cavern diameter of 14m and average cavern porosity of 16%, the time for one pore water exchange cycle, t, is calculated from:

$$t = \frac{\text{pore volume } (m^3) \text{ per } m^3 \text{ x the cavern diameter}}{\text{water flux}} = \frac{0.16 \text{ x } 14m}{4 \cdot 10^{-11} \text{ ms}^{-1}} = 5.6 \cdot 10^{10} \text{ s}$$

$$= 1.8 \cdot 10^3 \text{ years}$$

For the lower groundwater flow rate of $4 \cdot 10^{-13}$ ms^{-1}, t is $1.8 \cdot 10^5$ years and for the base case ($4 \cdot 10^{-12}$ ms^{-1}), $1.8 \cdot 10^4$ years.

However, modelling the averaged cavern type cements in this way is only a very simple way of comparing the overall behaviour: the batch or mixing tank approach takes no account of the real physical form of the repository and the distribution of the concrete therein, therefore, it is not possible to model heterogeneity in the system. This is potentially a very important problem because of the different permeabilities of the various concretes. It is possible that the high porosity backfill concrete will act as a conduit, channelling groundwater through a relatively small volume of the repository. This could have severe consequences in terms of the duration of the high pH conditions in this concrete type.

Table 12: Estimates of the lifetimes, in years, of the high pH (>11) conditions in the different repository components during degradation in Wellenberg groundwater for a range of water flow rates. These estimates represent minimum lifetimes as, under ideal circumstances, the infiltrating groundwater would initially react with the cavern lining cement and, therefore, be close to saturation with respect to the cement minerals when it passes into the backfill and other repository components. It is assumed that flow through the repository components is given by the average groundwater flux calculated from the geosphere hydraulic conductivity multiplied by a hydraulic gradient of 0.4. The shaded columns of the table indicate the estimates for the base case water flux using a geosphere hydraulic conductivity of 10^{-11} ms^{-1}. No account is taken of the hydraulic conductivity or actual disposition of the repository components (a standard 14m section across a cavern is assumed).

groundwater	**Wellenberg $NaHCO_3$ water**			**Wellenberg NaCl water**		
flow rate (ms^{-1})	**$4 \cdot 10^{-11}$**	**$4 \cdot 10^{-12}$**	**$4 \cdot 10^{-13}$**	**$4 \cdot 10^{-11}$**	**$4 \cdot 10^{-12}$**	**$4 \cdot 10^{-13}$**
Cavern backfill	$1.1 \cdot 10^6$	$1.1 \cdot 10^7$	$1.1 \cdot 10^8$	$7.7 \cdot 10^5$	$7.7 \cdot 10^6$	$7.7 \cdot 10^7$
Cavern lining	$4.2 \cdot 10^6$	$4.2 \cdot 10^7$	$4.2 \cdot 10^8$	$2.9 \cdot 10^6$	$2.9 \cdot 10^7$	$2.9 \cdot 10^8$
Cav. type 1 walls	$3.8 \cdot 10^6$	$3.8 \cdot 10^7$	$3.8 \cdot 10^8$	$2.6 \cdot 10^6$	$2.6 \cdot 10^7$	$2.6 \cdot 10^8$
Cav. type 1 waste	$3.5 \cdot 10^6$	$3.6 \cdot 10^7$	$3.6 \cdot 10^8$	$2.3 \cdot 10^6$	$2.3 \cdot 10^7$	$2.3 \cdot 10^8$
Cav. type 2/4	$3.4 \cdot 10^6$	$3.4 \cdot 10^7$	$3.4 \cdot 10^8$	$2.3 \cdot 10^6$	$2.3 \cdot 10^7$	$2.3 \cdot 10^8$

groundwater	Wellenberg $NaHCO_3$ water			Wellenberg NaCl water		
flow rate (ms^{-1})	$4 \cdot 10^{-11}$	$4 \cdot 10^{-12}$	$4 \cdot 10^{-13}$	$4 \cdot 10^{-11}$	$4 \cdot 10^{-12}$	$4 \cdot 10^{-13}$
Cavern type 1	$1.9 \cdot 10^6$	$1.9 \cdot 10^7$	$1.9 \cdot 10^8$	$1.4 \cdot 10^6$	$1.4 \cdot 10^7$	$1.4 \cdot 10^8$
Cavern type 2	$1.8 \cdot 10^6$	$1.8 \cdot 10^7$	$1.8 \cdot 10^8$	$1.3 \cdot 10^6$	$1.3 \cdot 10^7$	$1.3 \cdot 10^8$
Cavern type 3	$9.0 \cdot 10^5$	$9.0 \cdot 10^6$	$9.0 \cdot 10^7$	$5.4 \cdot 10^5$	$5.4 \cdot 10^6$	$5.4 \cdot 10^7$
Cavern type 4	$1.4 \cdot 10^6$	$1.4 \cdot 10^7$	$1.4 \cdot 10^8$	$1.1 \cdot 10^6$	$1.1 \cdot 10^7$	$1.1 \cdot 10^8$

Table 13: Estimates of the lifetimes, in years, of the high pH (>11) conditions during degradation of averaged cavern type cements in Wellenberg groundwater for a range of water flow rates. For each cavern type, it is assumed that groundwater flow is perpendicular to the cavern length, and the lifetimes are for the porewater in a 14m-long section of $1 m^2$ across the cavern diameter parallel to the water flow. The estimates in the shaded column are for the water flux calculated with the base case geosphere hydraulic conductivity of 10^{-11} ms^{-1} multiplied by the hydraulic gradient of 0.4.

As an illustration, consider the possible consequences of cracks in the cavern lining:

- The cavern lining is approximately 50 cm thick with a porosity of 6.4%, so the time for 1 pore water exchange cycle is 25 to 10000 years. (The low porosity of this concrete means that its hydraulic conductivity is also very low and times closer to the higher value are probably more realistic.) The duration of the high pH porewater is 2340 cycles corresponding to $5.9 \cdot 10^4$ - $2.4 \cdot 10^7$ years in $NaHCO_3$ water or 1600 cycles and $4 \cdot 10^4$ - $1.6 \cdot 10^7$ years in NaCl water.
- In contrast, the backfill concrete may constitute a slice through the repository up to about 13 metres long with a porosity of 24%. Using a higher water flux of 10^{-9} to 10^{-10} m^3/m^2s to take into account the higher hydraulic conductivity of this concrete gives a cycle time of 100 to 1000 years. The high pH porewater duration is only 590 cycles in $NaHCO_3$ water and 430 cycles in $NaHCO_3$ water or $5.9 \cdot 10^4$ - $5.9 \cdot 10^5$ years and $4.3 \cdot 10^4$ - $4.3 \cdot 10^5$ years, respectively.
- Under ideal circumstances, the groundwater will already be saturated or near saturated with respect to the cement minerals when it comes in contact with the backfill cement, having already passed through the cavern lining cement. Hence, the rate of degradation of the backfill cement will be limited by the slow degradation of the cavern lining cement and a high pH duration in excess of 10^6 years is likely. However, should cracks develop in the cavern lining, the incoming groundwater could be significantly undersaturated due to reduced contact with the cavern lining concrete resulting in much more rapid dissolution of the backfill cement. In this case, the duration of the high pH porewater is likely to be closer to that estimated, above, for the backfill concrete alone.

7 EVOLUTION OF THE REPOSITORY REDOX CONDITIONS

There is considerable interest in knowing how the redox conditions in a repository develop with time because of the influence of Eh on the solubility and sorption of the radionuclides. Although the problem is simply defined; the amounts of the oxidisable material in the repository are known quite accurately and the amounts of oxygen either enclosed initially, generated by radiolysis or present in groundwater can be estimated, the system is unlikely to exist in a state of homogeneous redox equilibrium. There are particularly problems with the influence of the H_2 gas evolved from anaerobic corrosion of the steel and other metals: in theory, it will buffer the Eh at a low value, in practice this is unlikely as the H_2O/H_2 system is very slow to attain equilibrium. Also, the effect of microbial action on the organic material in the repository is not amenable to simple calculations. What follows, therefore, is a brief assessment of the influence of the various parameters and an attempt to provide a semi-quantitative statement about the evolution of repository redox conditions.

7.1 Redox active materials in the repository

7.1.1 Metals

Metals, both waste and construction components, constitute a large source of oxidisable material in the repository. Steel, in the form of waste canisters, decommissioning waste and concrete reinforcing, is the major part of this constituting $9.5 \cdot 10^4$ tonnes (Table 14). Of less importance, due to either their corrosion behaviour or small inventory, are 390 tonnes of Al and Zn, 324 tonnes of "Zircaloy"[6], 1720 tonnes of "Inconel"[7] and also Pb in the waste.

7.1.2 Cement

Although GLASSER et al. (1990) report an oxidation capacity (i.e. the amount of oxidisable material) for OPC of 0.1 meq/g, it is difficult to account for it in terms of the normal chemistry of the cement. (Indeed, the authors suggest that it may be an artefact of the experimental technique.) Cement usually contains several percent of Fe-oxides but it is normally in the form of Fe_2O_3 and not ferrous oxides which could be further oxidised (TAYLOR 1990). Some ferrous oxides may be produced under reducing conditions during clinkering but it is re-oxidised on cooling as reduced oxides are considered detrimental to the quality of the cement. In this study, Fe in the cement is considered to be present as Fe_2O_3 or as Fe^{3+} in the hydrated minerals such

[6] Zirconium-based alloy (~98% Zr).
[7] Nickel-based alloy (50 to 70+ % Ni, depending on the particular alloy, with Cr, Fe, Ni, Mo and Ti)

as hydrogarnet. Thus, the oxidation capacity of the cement is zero. This is also assumed to be the case for all cement types.

Table 14: Material inventory of the waste groups SMA-1 to SMA-4 and the SMA repository total (NAGRA 1993b, table 2.2.8)

Material	SMA-1 (kg)	SMA-2 (kg)	SMA-3 (kg)	SMA-4 (kg)	Total (kg)
Metals					
Steels	$3.91 \cdot 10^7$	$8.82 \cdot 10^6$	$2.27 \cdot 10^6$	$7.50 \cdot 10^6$	$5.77 \cdot 10^7$
Al/Zn	$1.48 \cdot 10^5$	$1.01 \cdot 10^5$	$7.07 \cdot 10^4$	$6.92 \cdot 10^4$	$3.89 \cdot 10^5$
Inconel	$1.72 \cdot 10^6$	-	-	-	$1.72 \cdot 10^6$
Zircalloy	$3.24 \cdot 10^5$	-	-	-	$3.24 \cdot 10^5$
Other	$9.86 \cdot 10^5$	$4.87 \cdot 10^4$	$3.58 \cdot 10^4$	$7.4 \cdot 10^5$	$1.80 \cdot 10^6$
Total	$4.22 \cdot 10^7$	$8.97 \cdot 10^6$	$2.38 \cdot 10^6$	$8.31 \cdot 10^6$	$6.19 \cdot 10^7$
Inorganics					
Salts	$4.42 \cdot 10^4$	-	-	$1.78 \cdot 10^5$	$2.22 \cdot 10^5$
Ashes	$9.48 \cdot 10^4$	$2.68 \cdot 10^5$	-	$2.98 \cdot 10^4$	$3.93 \cdot 10^5$
Glass	$2.82 \cdot 10^3$	$4.68 \cdot 10^5$	$4.61 \cdot 10^5$	$6.77 \cdot 10^5$	$1.61 \cdot 10^6$
Concrete/cement	$1.25 \cdot 10^8$	$1.33 \cdot 10^7$	$5.40 \cdot 10^6$	$2.95 \cdot 10^7$	$1.74 \cdot 10^8$
Other	$8.06 \cdot 10^3$	$1.89 \cdot 10^6$	$5.79 \cdot 10^1$	$3.16 \cdot 10^4$	$1.93 \cdot 10^6$
Total	$1.26 \cdot 10^8$	$1.60 \cdot 10^7$	$5.86 \cdot 10^6$	$3.05 \cdot 10^7$	$1.79 \cdot 10^8$
Organics					
High molecular weight					
-Bitumen	-	-	-	$3.36 \cdot 10^5$	$3.36 \cdot 10^5$
-Ion exchange resins	$1.37 \cdot 10^6$	$6.27 \cdot 10^5$	-	-	$2.00 \cdot 10^6$
-Cellulose	$4.79 \cdot 10^1$	$2.96 \cdot 10^4$	$6.88 \cdot 10^4$	$5.67 \cdot 10^6$	$5.77 \cdot 10^6$
-Other	$2.11 \cdot 10^5$	$2.98 \cdot 10^5$	$7.37 \cdot 10^5$	$3.07 \cdot 10^6$	$4.32 \cdot 10^6$
subtotal	$1.58 \cdot 10^6$	$9.55 \cdot 10^5$	$8.06 \cdot 10^5$	$9.08 \cdot 10^6$	$1.25 \cdot 10^7$
Low molecular weight					
-Detergents	$3.81 \cdot 10^2$	$4.25 \cdot 10^4$	-	$9.41 \cdot 10^2$	$4.38 \cdot 10^4$
-Flocculants	-	$5.68 \cdot 10^2$	-	$6.35 \cdot 10^{-1}$	$5.69 \cdot 10^2$
-Complexing agents	-	$2.74 \cdot 10^4$	-	$2.89 \cdot 10^3$	$3.03 \cdot 10^4$
-Other	$8.32 \cdot 10^2$	-	-	$2.36 \cdot 10^2$	$1.07 \cdot 10^3$
subtotal	$1.21 \cdot 10^3$	$7.05 \cdot 10^4$	-	$4.07 \cdot 10^3$	$7.58 \cdot 10^4$
Total	$1.58 \cdot 10^6$	$1.03 \cdot 10^6$	$8.06 \cdot 10^5$	$9.09 \cdot 10^6$	$1.25 \cdot 10^7$
Not specified	$3.70 \cdot 10^3$	$8.51 \cdot 10^4$	-	$1.44 \cdot 10^5$	$2.33 \cdot 10^5$
Total	**$1.70 \cdot 10^8$**	**$2.60 \cdot 10^7$**	**$9.05 \cdot 10^6$**	**$4.80 \cdot 10^7$**	**$2.53 \cdot 10^8$**

7.1.3 Organic and other waste materials

In addition to organic waste, cellulose, plastics, ion exchange resins etc., which constitutes both a large source of oxidisable material and a nutrient source for microbial activity, the waste also contains quantities of ash from the incineration of some organic materials, and glass. While it is possible that the degradation of organics could influence the evolution of repository Eh (see below), the influence of the ash is more uncertain. The glass, being composed mainly of silica has no oxidation capacity and thus, no influence on Eh. The ash, however, may have a high carbon content possibly only partly oxidised due to incomplete incineration, and so may be further oxidised. In the following discussion the ash is not considered, on the assumption that any effect it does have will be beneficial, i.e. it will act as an oxygen sink.

7.2 Evolution of Eh

7.2.1 Aerobic phase of repository conditions

Initially the repository contains large volumes of air trapped in the concrete. After closure, water seeping in will displace some of this air and dissolve some of the oxygen from that remaining. During this time steel, aluminium and zinc, and organic material in the repository will be oxidised using up the enclosed oxygen. The duration of this aerobic phase will depend on the amount of oxygen enclosed and the rate of oxidation reactions. Based on the assumption that all the porosity in the repository is initially filled with air, WIBORGH et al. (1986) calculated that it would take 1-5 years to use up all the enclosed oxygen if it was only taken up by oxidation of steel with a high corrosion rate of 10^{-3} to 10^{-4} mm y^{-1}. If the oxygen was used only in oxidising Al, the aerobic stage would last 3 years and with cellulose, 1.5 years. These estimates neglect any consideration of transport between sites of oxidation (e.g. concentrated around the waste) and the surrounding volumes of the repository, being based purely on extrapolation of the initial corrosion rates. Also, the calculation was based on Fe oxidation to FeO(OH) which under anaerobic, high pH conditions will become unstable with respect to magnetite, Fe_3O_4.

Work by SHARLAND et al. (1986) predicts that fully anaerobic conditions (i.e. with an Eh around -700mV) buffered by hydrogen gas from anaerobic corrosion of the steel, could be achieved throughout the repository in approximately 100 years. This is based on modelling of the diffusion of hydrogen away from the corroding steel canisters and into the surrounding concrete matrix. It is likely to be a conservative estimate since it considers only the steel of the waste canisters and neglects the effect of the large amounts of structural (reinforcing) steel used throughout the repository. Also the model assumes that the Eh is buffered by the dissolved H_2 gas at -750mV (Eh given by the H_2O/H_2 half cell at pH = 12.5). It is unlikely, however, that the Eh will be so low because of the time taken to attain equilibrium between hydrogen and water. More likely is that Eh will be controlled by the balance of Fe^{3+}/Fe^{2+} at a level around -700mV (SHARLAND et al. 1986), perhaps locally heterogeneous with values depending on the distance from the sites of corrosion. This modelling study also ignores any microbial influence which could be important around organic waste materials.

Despite the order of magnitude differences in the results from the two studies, they serve to indicate that the early aerobic phase in the repository will be a brief, transitory stage of approximately 100 years, much less than the duration of one porewater exchange cycle (ca. 1000 years depending on the groundwater flow rate used).

7.2.2 Anaerobic phase of repository conditions

The duration of the anaerobic conditions will be determined primarily by the amount and corrosion rate of the steel. Aluminium and zinc are both present in the waste but in relatively small amounts compared to the large volumes of steel present in the repository. The corrosion rate for Al is 1000x higher than for steel and that for zinc 35x higher, therefore neither of these metals will effect the overall duration of the anaerobic conditions. Taking the maximum steel corrosion rate as 10^{-3} mm y^{-1} (GRAUER 1988; WIBORGH et al. 1986) and a surface area/volume ratio of 1000 m^2/m^3 (equivalent to a surface area/mass of 127 m^2 per tonne) the duration of the anaerobic conditions will be around 1000 years. With a more realistic corrosion rate of 10^{-4} - 10^{-5} mm y^{-1} (GRAUER et al. 1991), the expected lifetime is higher, around 10^4 - 10^5 years. Radiolytically produced oxygen will be present, mainly in the first 100 years, and oxygen may be present in the incoming groundwater. Although they will not significantly affect the steel oxidation rate at the high pH conditions, both of these sources could potentially affect organic waste degradation if they are not removed by metal oxidation.

7.2.3 Influence of radiolytic oxygen

The amount of radiolytic oxygen available for oxidation is around $1.25 \cdot 10^5$ moles over the first 500 years (derived from WIBORGH et al., 1986, p. 53, by scaling the underlying radionuclide inventory by a factor of *ca* 2). This is sufficient to oxidise 10.5 tonnes of steel to Fe_3O_4 over that period assuming the oxygen is not consumed by degradation of organic waste. This has no significant effect on the corrosion of the total steel inventory in the repository of around 100 000 tonnes.

7.2.4 Influence of groundwater oxygen

The input of oxygen into the system via the groundwater is potentially more important because of the large volumes of water involved. However, even if the amount of oxygen dissolved in the groundwater is assumed to be 0.1 mg dm^{-3} ($3 \cdot 10^{-6}$ mol dm^{-3}), the detection limit for analysis and therefore the maximum possible value as no dissolved oxygen was detected during the analysis, only 13 kg of steel are oxidised per porewater exchange cycle. As the expected lifetime of the steel is around 10^4 years which represents only tens of cycles, the oxidation of this amount of steel is trivial.

7.2.5 Degradation of organic materials

The rates for anaerobic microbial degradation of organic materials in the repository have large uncertainties; WIBORGH et al. (1986) cite 0.002 to 0.05 moles gas/kg.y for most organic materials and 0.05 to 0.7 moles gas/kg.y for cellulose. Despite the uncertainties, these rates indicate that organic matter could be still available for oxidation after 10^3 or even 10^4 years (see section 8.5 for more detail), the same time span as for the corrosion of the steel. If the lower rates of degradation pertain, the organic material could outlast the steel. In this case the repository Eh could be controlled by the microbial oxidation of the remaining organic matter. What the Eh would be under these circumstances is not known.

From these simple calculations it is clear that the radiolytic and groundwater oxygen do not constitute a significant threat to the duration of the low Eh conditions. The presence of substantial amounts of organic waste could aid the maintenance of the low Eh conditions if anaerobic microbial degradation proceeds slowly and the organic material outlasts the steel.

Without an influence from organic materials, the Eh will rise once all the steel is oxidised to Fe_3O_4. The Eh will be controlled initially by the reaction between Fe_3O_4 and ferric oxides, FeOOH or Fe_2O_3 until the magnetite is exhausted when the Eh will rise further to that of the incoming groundwater. The time for these last reactions and the rise of the Eh to ambient conditions has not been estimated.

8 INFLUENCE OF ORGANIC MATERIALS IN THE REPOSITORY

Degradation of organic materials in the repository by chemical processes or radiolysis or by microbial action could potentially have a large influence on the pH of the porewater because of the production of organic acids. The two main sources of organic material in the repository are:

- cement additives;
- waste materials (Table 14).

In view of the uncertainties in the type and amount of degradation products, and particularly in the degradation rates of many organic waste materials (see below), the calculations in the following sections aim to indicate the worst effects which could occur. In this way, the uncertainty involves only the potentially beneficial processes, such as incomplete degradation, loss of gaseous CO_2, etc.

8.1 Cement additives

Cement additives are used in the cement particularly to improve handling properties, e.g. to decrease the amount of water needed to produce adequate fluidity. These water reducers, or plasticisers and superplasticisers, are based mainly on four types of organic molecules:

- Ca or Na lignosulphonates or modified lignosulphonates;
- sulphonated naphthalene formaldehyde polymers;
- sulphonated melamine formaldehyde polymers;
- glucose-type polymers

Although the cement additives are used in the cement at quite low concentrations, up to 1.6 wt. % of the dry cement, their widespread occurrence throughout the cement means that they are a substantial source of organic material.

Glucose-type polymers are used at concentrations up to 0.8 wt.% dry cement. If we assume, in the absence of experimental or other evidence, that they are degraded by microbial action in a similar way to cellulose (see section 8.2.2) then 1 kg can degrade to produce at most 37 moles of gas of which half is CO_2 and half CH_4. Thus, the additive contained in 1 kg of dry cement could provide up to 0.3 moles of CO_2 which in turn provide 0.6 moles H^+ from the de-protonation of carbonic acid assuming that all CO_2 produced is eventually dissolved and none is lost as gas escaping from the repository. This is an unrealistic assumption but it allows an estimate of the maximum effect of the CO_2.

For comparison, the hydroxyl content of averaged cavern type 1 cement, for example, can be calculated from:

$$\text{Total hydroxyl content, } M_{OH} = M_{NaOH} + M_{KOH} + 2(M_{\text{"}Ca(OH)_2\text{"}} - M_{\text{"}SiO_2\text{"}})$$

where M_i is the number of moles of component i in 1 kg of dry cement;

and $2(M_{"Ca(OH)_2"} - M_{"SiO_2"})$ gives the number of moles of OH^- resulting from leaching of "$Ca(OH)_2$" from the initial CSH down to a C/S ratio of 1.0.

For averaged cavern type 1 cement: M_{NaOH} = 0.074 moles / kg of dry cement
M_{KOH} = 0.225 " "
$M_{Ca(OH)2}$ = 8.474 " "
M_{SiO2} = 4.021 " "

Therefore: M_{OH} = 9.2 moles / kg of dry cement

So complete degradation of the glucose polymers can potentially neutralise about 6% of the basic components of the cement.

The sulphonated melamine and naphthalene formaldehyde polymers (Figure 6) are used at higher concentrations, up to 1.6 wt. % dry cement in the waste cement formulations. If we assume that they are also broken down in a similar way to cellulose to ultimately yield gaseous products, 1 mole of sulphonated melamine formaldehyde ($C_3N_3(NHCH_2)_3OSO_3^-$), for example, could yield 6 moles CO_2 + 6 moles NH_3 + 1 mole H_2S. Such degradation products could also neutralise around 6% of the cement basic components.

If the rate of degradation of these additives is fast, the carbonic acid produced will neutralise predominantly KOH and NaOH resulting in very little change to the expected lifetime of the high pH pore water because these components contribute to the pH above 12.5. A slower rate of degradation, however, could result in carbonic acid neutralising "$Ca(OH)_2$" leached from the CSH gel. This would have a greater effect by directly reducing the amount of material available to buffer the high pH.

A

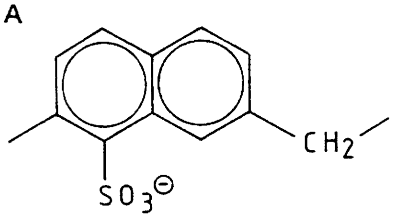

B

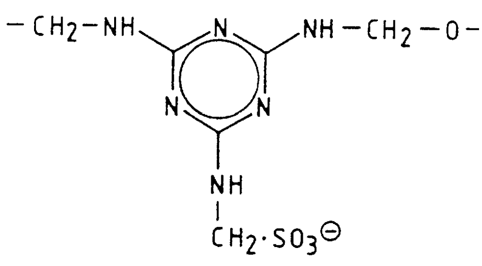

Figure 6: Repeating units which make up the structure of two cement additives: (A) - sulphonated naphthalene formaldehyde condensate and (B) - sulphonated melamine formaldehyde condensate. (TAYLOR 1990)

Although there are uncertainties about the rates and products of cement additive degradation, these estimates indicate that they represent a **significant** source of organic material, the acidic degradation products of which could react with the cement, impairing its ability to maintain a high porewater pH.

8.2 Organic waste

Like the cement additives, the organic waste components could produce significant amounts of acidic degradation products and affect the duration of the high pH pore fluid or locally reduce the pH. Because the waste is confined, the effects of its degradation may vary in intensity with proximity to the waste containers; it is envisaged that the waste matrix concrete will be severely affected. The organic waste materials include cellulose, polystyrene ion exchange resins, bitumen and other high molecular weight materials (plastics). In estimating the effects of the organic waste, the low molecular weight materials (detergents, flocculants etc.) have not been considered in detail: they are added to the inventory for high molecular weight organics. However, as overall they constitute less than 1% of organic waste and in SMA-1 this proportion is less than 0.1%, this contributes only a small inaccuracy.

8.2.1 Ion exchange resins

The ion exchange resins are composed of a framework of polystyrene-divinyl benzene with attached active groups, e.g. SO_3 for cation resin and $N(CH_3)_3$ for anion resin (NAGRA 1984). It has been suggested that the resins are degraded initially to C_8H_8 monomers with the loss of the functional groups, and that the monomers are further broken up to gaseous products (GROGAN 1987, cited in MUELLER-LEMANS 1990) according to the reaction:

$$C_8H_8 + 6\,H_2O \rightarrow 5\,CH_4 + 3\,CO_2$$

Hence, 1 mole of C_8H_8 could produce 3 moles of CO_2 and, from that 6 moles of H^+. Ion exchange resins contain approximately 26 wt.% functional groups in cation resins and 11 wt.% in anion resins (MUELLER-LEMANS 1990) so that 1 kg of dry cation resin contains 7.1 moles of C_8H_8 monomer which can yield 21.3 moles CO_2 and 42.6 moles H^+. For anion resin, 1 kg contains 8.6 moles C_8H_8 which can give 25.7 moles CO_2 and 51.4 moles H^+.

As the type of ion exchange resin is often not given in waste inventories, the higher CO_2 production value is used in the assessment of the effect of the degradation products.

8.2.2 Cellulose

The initial breakdown products of cellulose under high pH conditions are acids and aldehydes such as isosaccharinic, glycolic, lactic and formic acids and glycolaldehyde (VAN LOON 1992). On laboratory time-scales, these products appear quite stable and their ultimate fate, if they were formed in the repository, is not known. Theoretically, the anaerobic microbial degradation of cellulose produces only gas - 3 moles of CO_2 and 3 moles of CH_4 per mole of cellulose. Under experimental conditions, however, only about half of the expected amount of gas is produced and not of the predicted composition suggesting that this prediction is based on too simple a model and perhaps the early degradation reactions have some influence on the final products (WIBORGH et al. 1986). The maximum value of 6 moles gas / mole cellulose (37 moles gas /kg cellulose) has been used in the following calculations in spite of this uncertainty. This results in a maximum potential proton production of 37 moles H^+/kg cellulose.

8.2.3 Bitumen and other high molecular weight polymers

In an investigation of the radiolytic degradation of bitumen VAN LOON & KOPAJTIC (1990) found that the major products were monocarboxylic (acetic, formic, stearic etc.) and dicarboxylic (oxalic and phthalic) acids in addition to CO_2. However, these experiments were carried out in an oxidising atmosphere and it is not known whether similar products would result under anoxic conditions. It is possible that these organic acids could be produced during the initial oxic conditions when radiolysis is also at a maximum. The effect would be to reduce the amount of bitumen converted to CO_2 and CH_4. It is difficult to determine the total amount of organic acids which might be produced so, in the absence of other data, the value of 37 moles gas/kg organic material given by WIBORGH et al. (1986) has still been used for the degradation of bitumen and plastics as it gives a maximum CO_2 production.

8.3 The effect of organic degradation on SMA-1

For the waste group SMA-1, high sorption factors for cement are required for the radionuclides (NAGRA 1993b Table 2.2-2). These factors are influenced by pH and, in general, are higher with pH above 12 (see BRADBURY & SAROTT 1994). Therefore, faster degradation of the cement or a lower porewater pH may reduce the sorption in the repository and promote the dispersion of the radionuclides. Thus, the effect of the degradation products of the organic waste materials is particularly important in this repository type.

SMA-1 has less organic waste material than the other SMAs but the total inventory is still large comprising (from Table 14):

Ion exchange resins	1370	tonnes
Cellulose	0.05	tonnes
Low molecular weight materials	1.2	tonnes
Plastics and other high molecular weight materials	211	tonnes

The total organic waste material is $1.6{\cdot}10^3$ tonnes compared to a total amount of cement associated with the waste (i.e. matrix cement, container infill and walls and the cavern backfill) of $3.7{\cdot}10^4$ tonnes (Note: the value in Table 14 refers to cement **and concrete**, thus aggregate, which makes up over 80 wt.% of the backfill and container walls is also included.). The waste is listed in Table 15 by waste type with the total amount of H^+ its degradation products could provide. The total OH^- available in the waste matrix cement and in the surrounding concrete are also given for comparison. All the waste types listed will be in cavern type 1 and the available OH^- was calculated using cavern type 1 cement compositions: the waste matrix cement composition was used for the cement in the drums and the associated cement was the weighted average composition (proportions from Table 3) of the container infill, walls and backfill cements. Cavern type 1 waste matrix cement has an available OH^- content of 4.5 moles/kg of hydrated cement and the associated cement 6.8 moles/kg hydrated cement.

Comparing the amounts of OH^- available and H^+ potentially produced (Table 15), it is clear that the degradation products from the organic waste in several waste types (i.e. BA-KKB-1, BA-KKM-1, BA-KKG-1 and BA-KKL-1) could potentially neutralise all the available OH^- (as defined in section 8.1) in the waste matrix cement. In addition, the surrounding concrete could be affected. Using the CO_2 production values for the different waste types gives a total CO_2 production of $37 \cdot 10^6$ moles, yielding $78 \cdot 10^6$ moles H^+, for the organic waste in SMA-1.

Table 15: Hydroxyl availability in cement and potential H^+ production for organic waste types in SMA-1

Waste Types	Hydrated cement in drum (kg/drum)	Hydrated cement assoc.[1] (kg/drum)	OH^- available in cement in drum (moles/drum)	OH^- available in cement assoc. (moles/drum)	H^+-producing waste comp.[2]	H^+-producing waste amount (kg/drum)	H^+-producing waste potential H^+ (moles/drum)
BA-KKB-1	43	250	190	1700	1	60.2	3100
BA-KKB-3	222	500	1000	3400	1,3	6.5	265
BA-KKM-1	274	500	1230	3400	1	74.1	3810
BA-KKG-1	230	500	1030	3400	1	102	5240
BA-KKG-3	68	500	310	3400	3	2.0	80
BA-KKL-1	218	500	980	3400	1	40.0	2060
MIF-4	422	500	1900	3400	2,3	0.445	18

1: Cement around each waste container: including infill of repository containers, repository container walls and cavern backfill.

2: Composition of organic waste 1: Ion exchange resin
2: Cellulose
3: Other high molecular weight organics

In comparison, the total amount of cement contains $238 \cdot 10^6$ moles of OH^- (Calculated using the appropriate cement type for each of the associated cement components listed above, in the proportions given in Table 3. Cement associated with non-organic waste types are not included.). Thus, overall the degradation products can potentially neutralise about 30% of the cement basic components even in SMA-1 with a low content of organic material.

Thirty percent of the OH^- producing phases can be subtracted from the composition of averaged cavern type 1 cement in two ways:

1) by assuming that carbonic acid produced from CO_2 in the porewater would be neutralised first by the alkali hydroxide dissolution and then by portlandite and finally "$Ca(OH)_2$" from the CSH gel. This would probably be the result it organic degradation was fast, occurring predominantly within the first groundwater exchange cycle so that there were still abundant alkali hydroxides in the cement;
2) by assuming that carbonic acid produced from CO_2 in the porewater would be neutralised by portlandite and "$Ca(OH)_2$" from the CSH gel. This would be the

result of slow or delayed degradation of the organic material so that the production of CO_2 occurred mainly after alkali hydroxides and, perhaps also some of the portlandite, had been dissolved from the cement.

To illustrate the effect of these two scenarios on the duration of the high pH conditions, the degradation of averaged cavern type 1 cement (containing all the organics in SMA-1) was modelled:

Model 1:
the organic material was assumed to degrade totally within cycle 1. This has the effect of neutralising 30% of the cement OH^- before cycle 2. Averaged cavern type 1 cement is relatively high in alkalis and portlandite so that these phases are subtracted but the CSH gel composition is unaffected (Table 16). Hence, when this modified composition is used for normal groundwater cement degradation with DISSOLVE, there is only a small change to the number of cycles before the pH falls below 11.0: 1010 cycles instead of 1070 cycles (Figure 7).

Model 2:
the organic material is assumed to degrade totally within cycle 10 (when the alkali hydroxides and some portlandite have already been dissolved). This has the effect of neutralising 38% of the remaining cement OH^- before cycle 11. As can be seen in Table 16, this results in a change to the composition of the CSH phase and a sudden drop in the Ca in solution (Figure 7). However, it has very little effect on the overall lifetime of the high pH porewater: there are 1000 cycles before the pH falls below 11.0.

The reaction of cement $Ca(OH)_2$ with HCO_3^- results in precipitation of calcite. It was assumed in model 2 that almost all the Ca liberated from the cement would be precipitated as calcite in cycle 10. Although this doesn't result in a significant decrease in porosity (because the CH and CSH are dissolved) it does have an effect over the life of the system because a greater proportion of the Ca is converted into calcite. Therefore, the porosity and the volume of porewater is slightly smaller at any given cycle, than in the case of the normal organic-free degradation. This counteracts

Table 16: Composition of the averaged cavern type 1 cement before and after loss of OH^- content due to reaction with acidic degradation products of organic waste. Model 1 estimates the effect of organic degradation in the first cycle, and Model 2, organic degradation in cycle 10 after dissolution of most of the KOH and NaOH from the cement.

Moles / kg hydrated cement	**Cavern Type 1 (no organics)**	**Cavern Type 1 (model 1)**	**Cavern Type 1 (model 2)**
C_3FH_6	0.174	0.174	0.174
C_3AH_6	0.182	0.182	0.182
$C_{1.8}SH_{1.8}$	2.449	2.449	-
$C_{1.67}SH_{1.67}$	-	-	2.449
$C_6A\overline{S}_3H_{32}$	0.062	0.062	0.062
$Ca(OH)_2$	0.753	0.003	0.0
M_4AH_{10}	0.048	0.048	0.048
KOH	0.137	0.0	0.0
NaOH	0.045	0.0	0.0
Available OH^-	**5.606**	**3.924**	**3.288**

the effect of the diminished C/S ratio in the CSH gel which would otherwise have resulted in a significantly earlier fall in the pH. However, it should be noted that this result is very sensitive to model assumptions, in particular, the proportion of Ca converted to calcite in cycle 10; over 1000 or so cycles, small differences in porosity can produce a wide range of results.

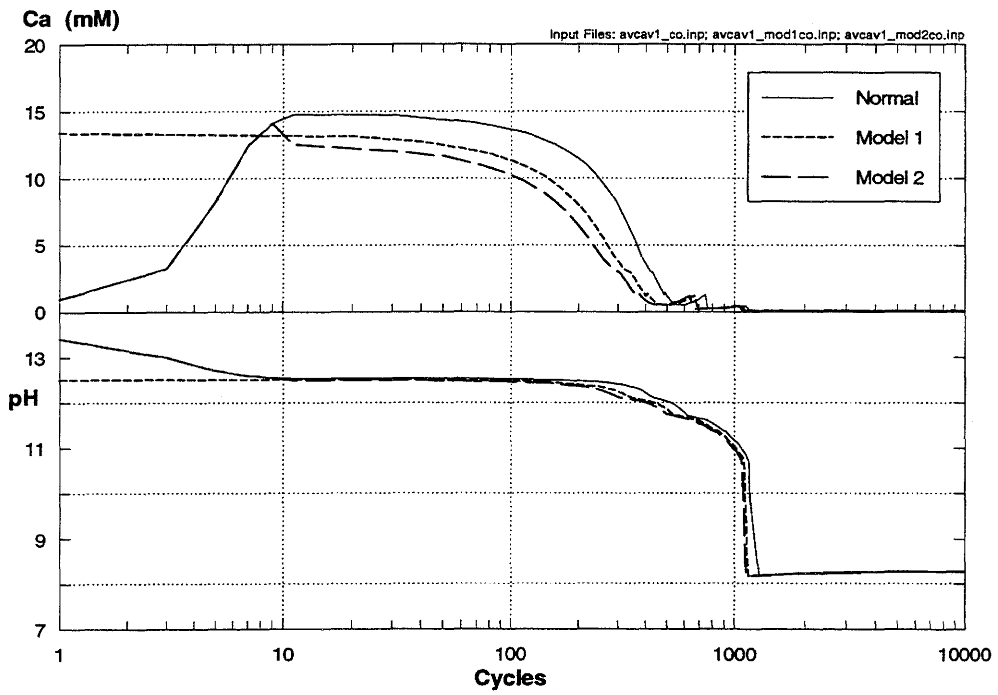

Figure 7: The effect of organic degradation products on the degradation of cement and the duration of high pH porewater in SMA-1 (averaged cavern type 1 cement in Wellenberg $NaHCO_3$ water)
Normal: undisturbed cement degradation (no organics);
Model 1: 30% of cement OH^- neutralised in cycle 1 (see text for details);
Model 2: 38% of remaining cement OH^- neutralised in cycle 10, after loss of the KOH and NaOH.

In model 1, much less Ca is dissolved and more K and Na so that a high ionic strength $(K,Na)CO_3$ solution results with proportionately less calcite precipitation and, thus, slightly higher porosity than in the normal case.

A rough estimate of the amounts of cement OH^- available in each waste group (SMA-1 to -4) and the corresponding maximum amount of H^+ which could be generated from the corresponding included waste is given in Table 17. The total cement volume for each SMA is divided into that in which the waste is incorporated (this also includes the cement in which non-organic waste is incorporated), the surrounding repository containers and backfill (also including cement associated with non-organic wastes), and the cavern lining. In contrast to SMA-1, which overall has sufficient cement in the waste volume alone to neutralise all the potential H^+ production from the organic waste in this section of the repository, SMA-2 and SMA-3 are likely to experience early loss of high pH conditions in the waste and also in the concrete most immediately associated with the waste packages. In SMA-4, however, there is hardly sufficient cement in the entire repository sector to overcome the effect of the organic waste degradation products. Even though this estimate is based on very conservative assumptions for both the organic waste degradation and the concrete (OPC + PFA) OH^- content, it is enough to illustrate that high pH conditions can not be ensured for this waste group and that safety considerations must rely on processes other that radionuclide sorption. In addition, the early loss of the high pH pore fluid could accelerate the corrosion of the steel canisters and affect the maintenance of low Eh conditions.

Table 17: Comparison of the availability of OH^- in cement and concrete and potential H^+ production from organic waste in the waste groups SMA-1 to SMA-4.

	OH^- available (moles) from concrete			H^+ arising from waste	
Waste Group	Cavern lining (1)	Backfill & containers	Waste	Organics (kg)	H^+ (mol) (7)
SMA-1	$2.8 \cdot 10^8$	$3.6 \cdot 10^8$ (2)	$1.8 \cdot 10^8$ (4)	$1.6 \cdot 10^6$	$7.8 \cdot 10^7$
SMA-2	$4.6 \cdot 10^7$	$6.0 \cdot 10^7$ (2)	$1.9 \cdot 10^7$ (4)	$1.0 \cdot 10^6$	$4.7 \cdot 10^7$
SMA-3	$1.8 \cdot 10^7$	$2.2 \cdot 10^7$ (2)	$2.4 \cdot 10^7$ (5)	$8.1 \cdot 10^5$	$3.0 \cdot 10^7$
SMA-4	$1.4 \cdot 10^8$	$2.0 \cdot 10^8$ (3)	$1.2 \cdot 10^7$ (6)	$9.1 \cdot 10^6$	$3.4 \cdot 10^8$

Notes:

(1) Based on total cavern lining volume of 115 900 m^3 for the SMA repository, divided by waste group according to the volume percentages in Table A2 (Appendix A). Cement and concrete composition from Tables 4 and 5.

(2) Based on a total SMA repository volume of 414 000 m^3 distributed between waste groups according to Table A2 (Appendix A), and subtracting waste volume (from NAGRA 1993b, Table 2.2-6) and cavern lining volume (note 1). OH^- content based on 450 kg hydrated cement per m^3 concrete (SMA-1 and SMA-2) or 420 kg hydrated cement per m^3 concrete (SMA-3) and 7 moles OH^- per kg hydrated cement.

(3) Volume as note 2, above. OH^- content based on 700 kg hydrated cement per m^3 concrete and 5 moles OH^- per kg hydrated cement.

(4) Based on waste cement/concrete contents from Table 14. OH^- content based on 0.2 kg hydrated cement per kg concrete and 7 moles OH^- per kg hydrated cement.

(5) Based on waste cement/concrete contents from Table 14. OH^- content based on 1.0 kg hydrated cement per kg concrete (no aggregate) and 4.5 moles OH^- per kg hydrated cement.

(6) Based on waste cement/concrete contents from Table 14. OH^- content based on 1.0 kg hydrated cement per kg concrete (no aggregate) and 0.4 moles OH^- per kg hydrated cement.

(7) Based on 51 moles H^+ per kg of ion exchange resin and 37 moles H^+ per kg of other organics. Organics contents from Table 14.

8.4 Rate of degradation of organic material

If the rate of organic degradation is greater than the dissolution of the cement, the pH of the pore fluid could fall. However, there is little data available for the rate of ion exchange resin or bitumen degradation. A gas production rate for organic materials, including bitumen, plastics and ion exchange resins, of 0.002 to 0.05 moles gas/kg.y, and 0.05 to 0.7 moles gas/kg.y for cellulose, is given by WIBORGH et al. (1986). Using the maximum rates and assuming they remain constant over a long time period, these organic materials could degrade in less than 750 years. This is of the same order of magnitude as the time for one porewater exchange cycle in the repository. If the H_2CO_3 is neutralised by alkalis and CH from the cement as it forms, it represents a high rate of cement degradation compared to the normal dissolution in the groundwater. It is possible that dissolution of the cement would not proceed sufficiently fast to supply the OH^- to maintain a high pH. Especially within the confines of a waste container, the pH may fall because of both the high local concentration of degrading waste and also, the difficulty of augmenting the supply of OH^- from the surrounding cement due to restricted water movement into the drum or container. Falling pH in the waste drums may in turn affect the corrosion of the steel; reducing the passivating effect of the magnetite and increasing the corrosion rate (GRAUER, 1988).

8.5 Calcite precipitation from cement neutralisation

A side product of the neutralisation reactions between carbonic acid from the degradation of the organic materials and the portlandite (and "$Ca(OH)_2$") from the cement is calcite. Even without the extra carbonate from the organic material breakdown, the $NaHCO_3$ groundwater precipitates some 80 mol.% of the calcium from the dissolution of the cement phases as calcite or mixed cation carbonates such as magnesian, strontian or ferroan calcite. With a porewater which can be kept saturated with carbonate because of the presence of excess CO_2 gas, the amount of calcium and other cations precipitated as carbonate minerals should increase. In theory, all of the Ca, Mg, Sr and Fe^{2+} from cement and groundwater (for the first few cycles) could be precipitated as minerals for many cavern/waste types because of the large amounts of CO_2 produced. Luckily, calcite and other carbonates are denser than the hydrated cement minerals so there is no question of a net increase in volume of the solid phase. However, the carbonate minerals will not necessarily precipitate in the same place as the cement minerals dissolve. Also, at low temperatures carbonate minerals commonly precipitate as concretionary bodies, preferring to grow on a pre-existing carbonate substrate rather than precipitate uniformly through a body of rock. Hence, there is a possibility that cement dissolution and carbonate mineral precipitation could profoundly modify the porosity and permeability distribution in the repository. As this aspect of cement degradation was not studied, it is uncertain whether this phenomenon is likely to be detrimental or favourable to the operation of the repository.

8.6 Degradation of organic materials - conclusion

There are great uncertainties on numbers in the foregoing discussion because much relies on assumptions of unknown validity. In general, much more information is needed about the longterm degradation of organic materials, particularly with regard to intermediate degradation products and degradation rates. However, the discussion serves to illustrate the potential effects of degrading organic materials in the repository. It also indicates that for some waste groups it is reasonable to expect long-lasting high pH conditions; even the worst case of organic degradation and subsequent reaction does not substantially impair the ability of the cement to maintain the pH above 11.0 in SMA-1. For SMA-4 the situation is much more uncertain. The large amounts of cellulose and the lower acid buffer capacity of the waste cement suggest that the pH will fall within the waste containers quickly ($<10^3$ years) and that the pH of the porewater throughout this repository section will fall more rapidly than in the other repository types.

9 CONCLUSIONS

- Modelling of the undisturbed SMA repository system (neglecting influences of waste etc.) for averaged cavern cements 1, 2 and 4, indicates that high pH conditions (pH > 11) could be maintained for about 700 cycles in NaCl groundwater and about 1000 cycles in $NaHCO_3$ groundwater. The less favourable composition of averaged cavern type 3 cement could result in pH falling below 11.0 at about 500 cycles in $NaHCO_3$ water and 300 cycles in NaCl water. For a host rock hydraulic conductivity of 10^{-11} ms^{-1}, one cycle corresponds to more than 1000 years.
- In the undisturbed system high pH duration is dependent on:
  - cement/concrete porosity
  - composition of the infiltrating groundwater
  - cement composition only for high blending agent content.
- The redox conditions (Eh) of the SMA repository will be dominated by anaerobic corrosion of the steel. The initial aerobic conditions will probably be very short, less than 100 years. The expected lifetime of the steel under anaerobic oxidation conditions is 10^3 to 10^5 years. Neither radiolytic oxygen nor incoming groundwater are likely to substantially reduce this period. The influence of the cement is limited as it is generally fully oxidised and takes no direct part in the redox reactions. When all the steel is oxidised, the Eh in the repository will rise gradually to that of the incoming groundwater, buffered by magnetite.
- Degradation of cement additives could neutralise in the worst case approximately 5% of the basic components of the cements in which they are used.
- Organic materials in the waste can have a significant influence on the chemical environment of the repository. Acidic degradation products of organic materials could neutralise significant proportions of basic components in cement.

However, the extent of the effects are difficult to calculate due to uncertainty about products and rates of organic degradation.

- Even on the basis of conservative assumptions about organic degradation products, SMA-1 is unlikely to experience a significant reduction in the duration of high pH conditions. This is true for both extremes of organic degradation rate which were evaluated. For SMA-2 and -3 the effect of organic degradation products will be greater due to the larger organic waste inventory; in both of these SMAs early loss of high pH conditions within the waste is expected with probably some effects extending to the surrounding concrete volume especially in SMA-3. For waste group SMA-4, the high organic content and the low OH^- content of the waste cement suggest the duration of high pH conditions will be severely affected.
- In all SMA types, areas of lower pH around the organic waste are to be expected as degradation rates of organic materials are likely to be significantly greater than that of cement. Falling pH in the waste concrete may result in increased corrosion of the steel which may in turn lead to earlier rise of Eh in the repository and higher gas production rates.

10 RECOMMENDATIONS FOR FURTHER WORK

Aspects of the cement degradation model could be improved by:

- addition of a mechanism to describe the incongruent dissolution of hydrotalcite;
- inclusion of Fe in the model;
- removal of the hydrogarnet $LogK_{sp}$ restriction;
- addition of thermodynamic data to allow modelling at higher temperature.

However, the effects of the first three would be very minor, they represent fine tuning of the model, and the last suggestion is difficult because of the lack of good experimental data on the dissolution of the CSH phase at temperatures above 25°C. In view of the uncertainties in other important aspects of the near-field system, such as the longterm degradation of the organic waste and cement additives, which introduce much larger variations, further refinement of the cement degradation model is not justified for the present application. For other applications, for example, interaction of cement with the surrounding host rock, further refinement of the cement degradation model may be considered necessary.

However, two ways in which the degradation modelling could be advanced and which could provide valuable insights irrespective of the state of uncertainty over organic degradation, are:

1. the consideration of sequential degradation of the different cement types to simulate the effect of groundwater flowing through the various parts of the repository from one concrete to another;
2. the consideration of the effects of the calcite, and other secondary mineral, precipitation on the hydraulic properties of the concrete systems.

In particular, the combination of transport aspects with the chemistry should allow a much more realistic prediction of the duration of the high pH porewater by understanding something about the development of heterogeneity in the system. While neither of the above are trivial problems, they perhaps represent relatively well defined systems amenable to the application of current coupled codes.

11 ACKNOWLEDGEMENTS

I should like to thank, first of all, Dr. U. Berner for initiating me into the mysteries of cement chemistry and for many hours of valuable discussion on the topic thereafter; Dr. D. Macphee, Prof. R. Grauer and Dr. J. Pöttinger critically reviewed the manuscript which resulted in great improvements for which I hope the reader will also be grateful. I must further acknowledge Dr. Pöttinger in his role as NAGRA project co-ordinator for establishing this fruitful co-operation. The financial support of NAGRA for this work is gratefully acknowledged.

12 REFERENCES

ALDER J.C. & McGINESS D. (1994): Model radioactive waste inventory for Swiss waste disposal projects. Nagra Technical Report NTB 93-21. Nagra, Wettingen, Switzerland.

ATKINS M., BENNETT D., DAWES A., GLASSER F.P., KINDNESS A. & READ D. (1992): A thermodynamic model for blended cements. DoE Report Nr. DoE/HMIP/RR/92/005.

BERNER U. (1987): Modelling porewater chemistry in hydrated cement. Mat. Res. Soc. Symp. Proc., 84, 319.

BERNER U. (1990): A thermodynamic description of the evolution of pore water chemistry and uranium speciation during degradation of cement. PSI Bericht Nr. 62. Paul Scherrer Institute, Villigen, Switzerland.

BERRY E.E., HEMMINGS R.T., LANGLEY W.S. AND CARETTE G.G (1989): Beneficiated fly ash: hydration, microstructure and strength development in portland cement systems. Proc. 3rd Int. Conf. on Fly Ash, Silica Fume, Blast Furnace Slag and Natural Pozzolans, ACI SP114 - 11, 241-73.

BRADBURY M.H. & SAROTT F.-A. (1994): Sorption databases for the cementitious near field of a L/ILW repository for performance assessment. Nagra Technical Report NTB 93-08 in preparation. Nagra, Wettingen, Switzerland.

D'ANS J. & EICK H. (1953): Das System CaO-Al_2O_3-H_2O bei 20°C und das Erhärten der Tonerdezemente. Zement-Kalk-Gips, **6**, 197-210.

GLASSER F.P., ATKINS M., KINDNESS A., POINTER C., COWIE J., JAPPY T., MACPHEE D., BECKLEY N., CARSON S., WILDING C.R., MATTINGLEY N.J., EVANS P.A. & MCHUGH G. (1990): Characterisation and modelling of blended cements and their application to radioactive waste immobilization. DoE Report Nr. DoE/HMIP/RR/90/062.

GRAUER R. (1988): The corrosion behaviour of carbon steel in Portland cement. Nagra Technical Report NTB 88-02E. Nagra, Wettingen, Switzerland.

GRAUER R., KNECHT B., KREIS, P & SIMPSON J.P. (1991): Die Langzeit-Korrosiongeschwindigkeit des Eisens in anaeroben alkalischen Lösungen. Werkstoffe und Korrosion, **42**, 637-642.

GROGAN H.A. (1987): The significance of microbial activity in a deep repository for L/ILW. Nagra unpublished report. Nagra, Wettingen, Switzerland.

LEA F.M. (1970): The Chemistry of Cement and Concrete. Edward Arnold Ltd., London (Third edition).

JACOBS F., MAYER G. & WITTMANN F.H. (1994): Hochpermeable zementgebundene Verfüllmörtel für schwach- und mittelaktive Endlager. Nagra Technical Report NTB 92-11. Nagra, Wettingen, Switzerland.

JONES F.E. & ROBERTS M.H. (1962): The system $CaO\text{-}Al_2O_3\text{-}H_2O$ at 25 degrees C. DSIRO Building Research Station Note 965, Watford, Herts.

KOMURKA M. & SCHEIBER R (1989): Hydrolytische Gleichgewichte von Hydraten des Portlandzementes 1. Teil. Oesterreichisches Forschungszentrum Seibersdorf Ges.m.b.H OEFZS-4497.

MASCOLO G. & MARINO O. (1980): A new synthesis and characterisation of magnesium-aluminium hydroxides. Min. Mag., **43**, 619-21.

MÜLLER-LEMANS H. (1990): Berechnungen zur pH- und pe-Pufferung im Betriebsabfall von Kernkraftwerken. Nagra unpublished report. Nagra, Wettingen, Switzerland.

NAGRA (1984): Inventar und Charakterisierung der radioaktiven Abfälle in der Schweiz. Nagra Technical Report NTB 84-47. Nagra, Wettingen, Switzerland.

NAGRA (1993a): Endlager für kurzlebige Abfälle: Technische Berichte zum generellen Projekt SMA-AB:
- Anlagen unter Tag;
- Container und Transporte;
- Endlagerbetrieb.

Nagra unpublished reports. Nagra, Wettingen, Switzerland.

NAGRA (1993b): Beurteilung der Langzeitsicherheit des Endlagers SMA am Standort Wellenberg (Gemeinde Wolfenschiessen, NW). Nagra Technical Report NTB 93-26. Nagra, Wettingen, Switzerland.

NAGRA (1993c): Untersuchungen zur Standorteignung im Hinblick auf die Endlagerung schwach- und mittelaktiver Abfälle. Geologische Grundlagen und Datensatz zur Beurteilung der Langzeitsicherheit des Endlagers SMA am Standort Wellenberg (Gemeinde Wolfenschiessen, NW). Nagra Technical Report NTB 93-28. Nagra, Wettingen, Switzerland.

NAGRA (1994): Rahmenbewilligungsgesuch. Endlager für kurzlebige schwach- und mittelaktive Abfälle (Endlager SMA). Bericht zur Langzeitsicherheit des Endlagers SMA am Standort Wellenberg (Gemeinde Wolfenschiessen, NW). Nagra Technical Report NTB 94-06. Nagra, Wettingen, Switzerland.

PEARSON F.J. & BERNER U. (1991): Nagra thermochemical database: I. Core data. Nagra Technical Report NTB 91-17. Nagra, Wettingen, Switzerland.

PEARSON F.J., BERNER U. & HUMMEL W. (1992): Nagra thermochemical database: II. Supplemental data 05/92. Nagra Technical Report NTB 91-18. Nagra, Wettingen, Switzerland.

REARDON E.J. (1990): An ion interaction model for the determination of chemical equilibria in cement/water systems.Cement and Concrete Research, **20**, 175-92.

SHARLAND S.M., TASKER P.W. & TWEED C.J. (1986): The evolution of Eh in the pore water of a model nuclear waste repository. AERE R 12442, Harwell, Oxon.

TAYLOR H.F.W. (1990): Cement Chemistry. Academic Press Inc., San Diego, CA.

TURRIZIANI R. (1964): The calcium aluminate hydrates and related compounds. In The Chemistry of Cements, vol.I (ed. M.F.W Taylor), Academic Press, London.

VAN LOON L. (1993): The alkaline degradation of cellulose and cellulose derivatives: Impact on radionuclide speciation. PSI Internal Technical Report TM-43-92-45. Paul Scherrer Institute, Villigen, Switzerland.

VAN LOON L. & KOPAJTIC Z. (1990): Complexation of Cu^{2+}, Ni^{2+} and UO_2^{2+} by radiolytic degradation products of bitumen. PSI-Bericht Nr. 66. Paul Scherrer Institute, Villigen, Switzerland.

VIEILLARD P. & RASSINEUX F. (1992): Thermodynamic and geochemical modelling of the alteration of two cement matrices. Applied Geochemistry. Suppl. Issue No.1,125-136.

WIBORGH M., HÖGLUND L.O. & PERS K. (1986): Gas formation in a L/ILW repository and gas transport in the host rock. Nagra Technical Report NTB 85-17. Nagra, Wettingen, Switzerland.

WOLERY T.J., 1983: EQ3NR. A Geochemical aqueous speciation - solubility code. UCRL-53414 Lawrence Livermore National Laboratory, Livermore, California.

ZHANG F., ZHOU Z. & LOU Z. (1980): Solubility product and stability of Ettringite. 7th Int. Congr. Chem. Cem., II, Theme 2, 88-93.

APPENDIX A

SMA-1	BA RA SA MIF WA	BA-1, BA-3, BA-6 RA-1, RA-4, RA-5, RA-6, RA-7 SA-KKW-1, SA-KKW-2..6, SA-PSIW MIF-4
SMA-2	BA RA SA MIF WA	 SA-KKW-8 MIF-1, MIF-2, MIF-3A, MIF-5B
SMA-3	BA RA SA MIF WA	BA-5 MIF-5A
SMA-4	BA RA SA MIF WA	BA-2 SA-KKW-7 MIF-3B WA-5

Table A-1: Allocation of the different waste types to the different SMA waste groups (c.f. NAGRA 1993b, table 2.2-5)

Waste Group	**Cavern segments**			
	Type-1	**Type-2**	**Type-3**	**Type-4**
SMA-1	8.7	49.4	-	-
SMA-2	5.0	4.4	-	-
SMA-3	3.8	-	-	-
SMA-4	1.5	3.3	17.5	6.4

Table A-2: Volume percentages of the different cavern segment types in the four waste groups making up the SMA repository. The allocation of waste types to the waste groups is as Table A-1, and the volumes of individual waste types is taken from ALDER & McGINNES (1994).

APPENDIX B

Results of the cement degradation modelling for individual cement compositions (Figs B-1 to B-10) and for averaged cavern type cements (Figs B-11 to B-18).

The cement degradation model incorporated in DISSOLVE simulates the results of a batch experiment in which 1kg of hydrated cement reacts to equilibrium with successive aliquots of groundwater. The volume of water in each cycle corresponds to the pore volume of the 1kg sample and changes throughout the experiment as cement phases dissolve and secondary minerals, e.g. calcite, are precipitated. The pore water composition, pH, porosity and remaining solid phase composition at selected cycles are included in the output from the program. The following figures show the evolution of pore water composition and pH with increasing number of water exchange cycles. Degradation modelling has been carried out for two Wellenberg groundwaters ($NaHCO_3$ water and NaCl water).

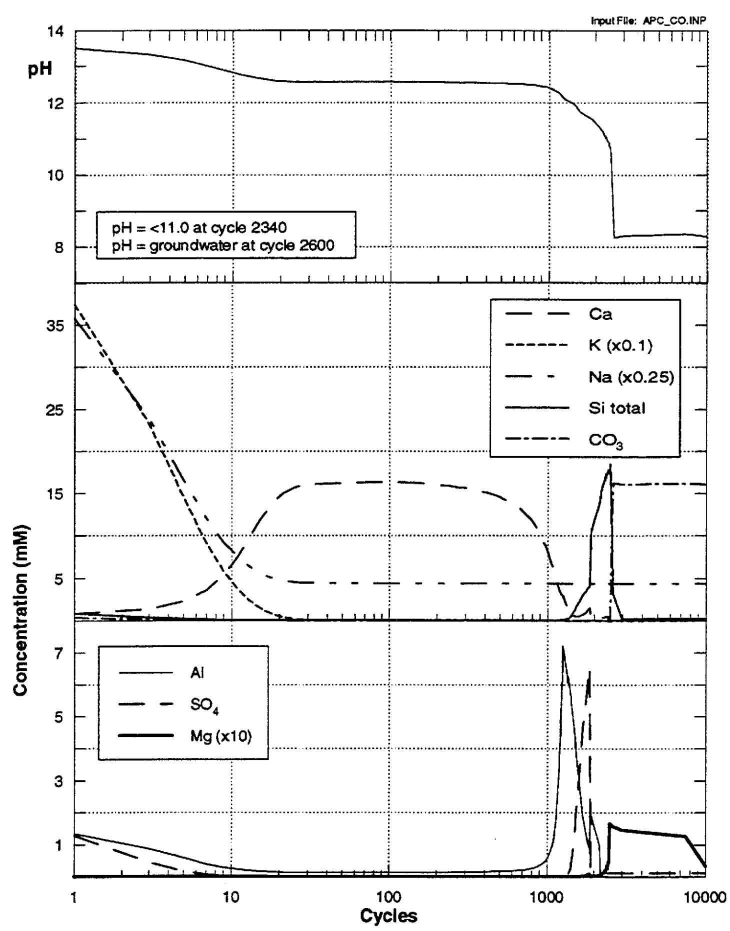

Figure B-1: Results of the cement degradation modelling for cavern lining cement (average Swiss Portland cement) in Wellenberg $NaHCO_3$ water.

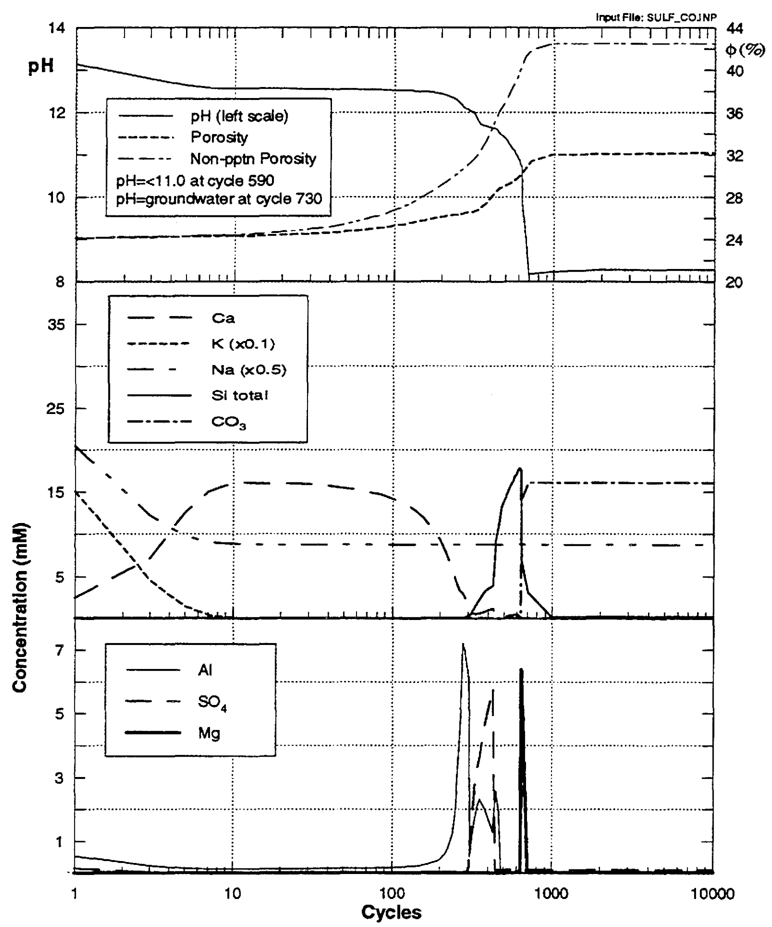

Figure B-2: Results of the cement degradation modelling for cavern backfill cement (Sulfacem modelled with 24% concrete porosity) in Wellenberg $NaHCO_3$ water. Non-pptn porosity is the normal porosity plus the volume of the secondary, precipitated minerals such as calcite. It is explained in more detail in section 5.

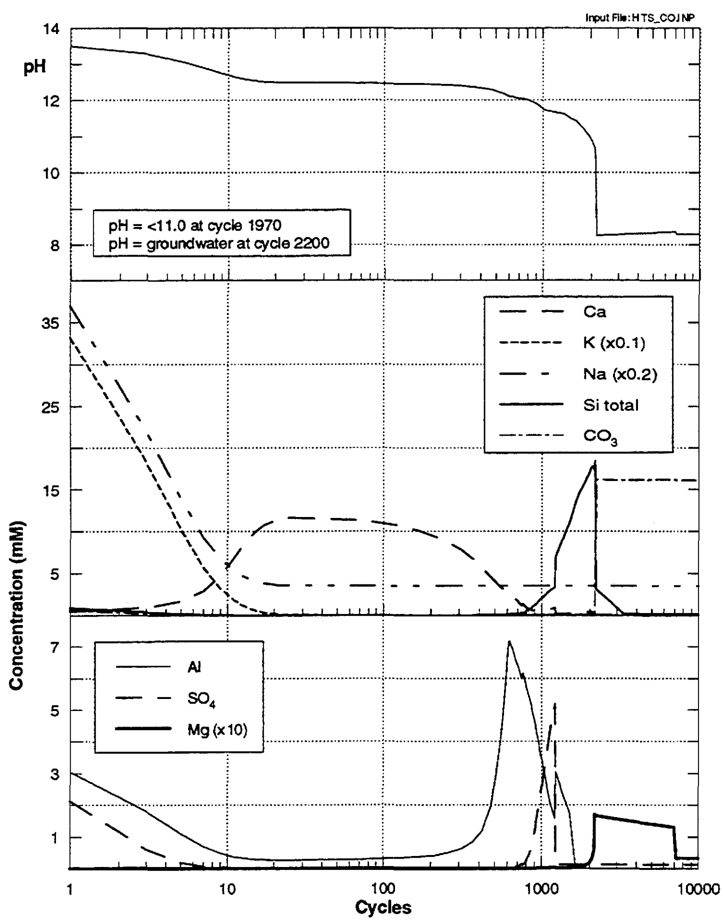

Figure B-3: Results of the cement degradation modelling for cavern type 1 waste cement (HTS plus trass) in Wellenberg $NaHCO_3$ water

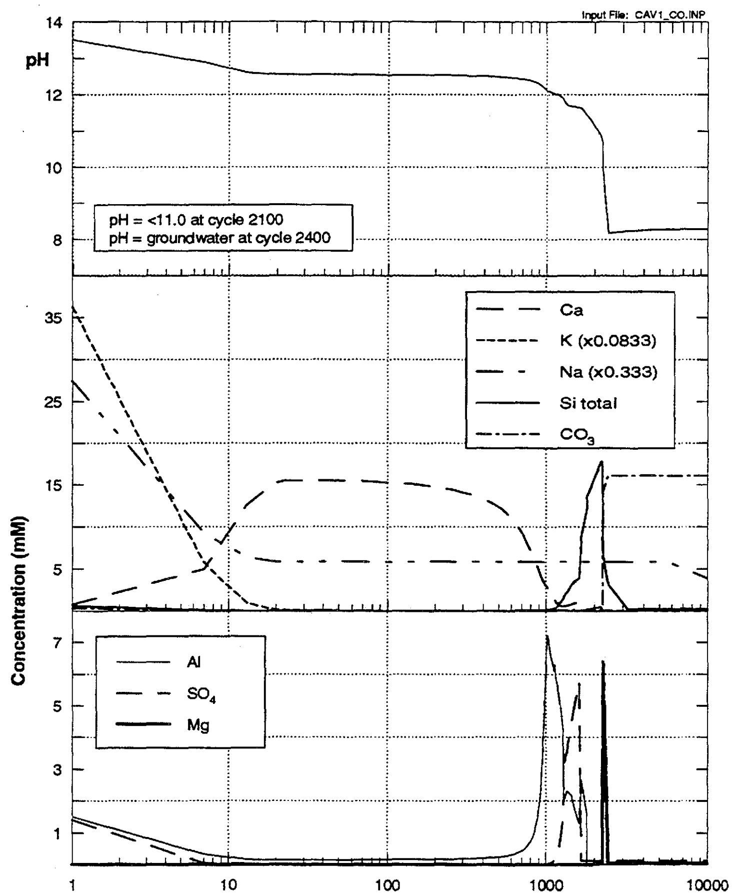

Figure B-4: Results of the cement degradation modelling for cavern type 1 container walls cement (Sulfacem with minimum porosity) in Wellenberg $NaHCO_3$ water

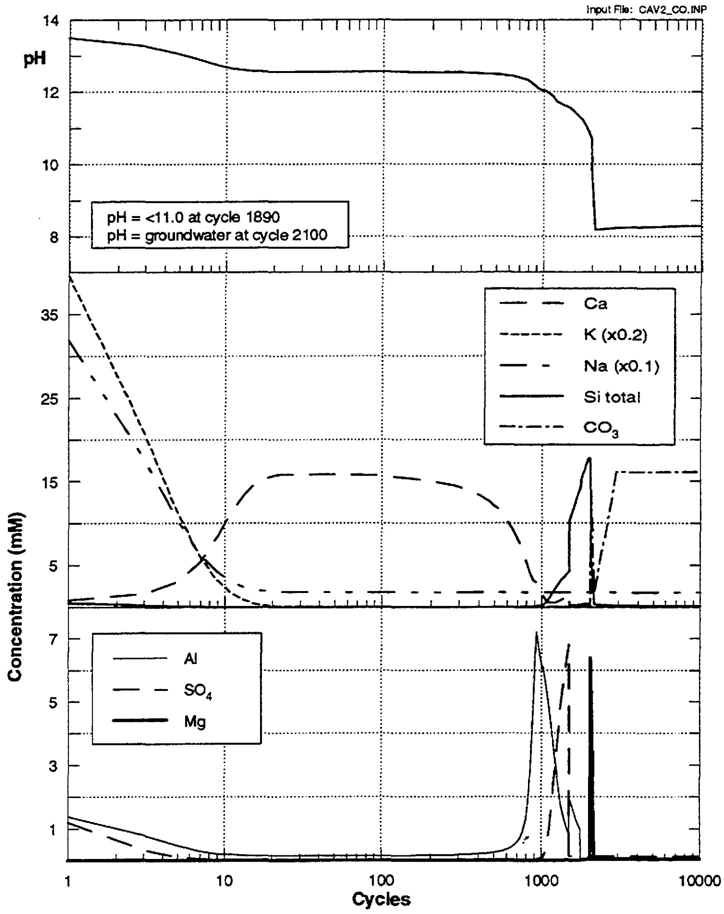

Figure B-5: Results of the cement degradation modelling for cavern type 2 container infill and walls cement (ordinary Portland cement) in Wellenberg $NaHCO_3$ water

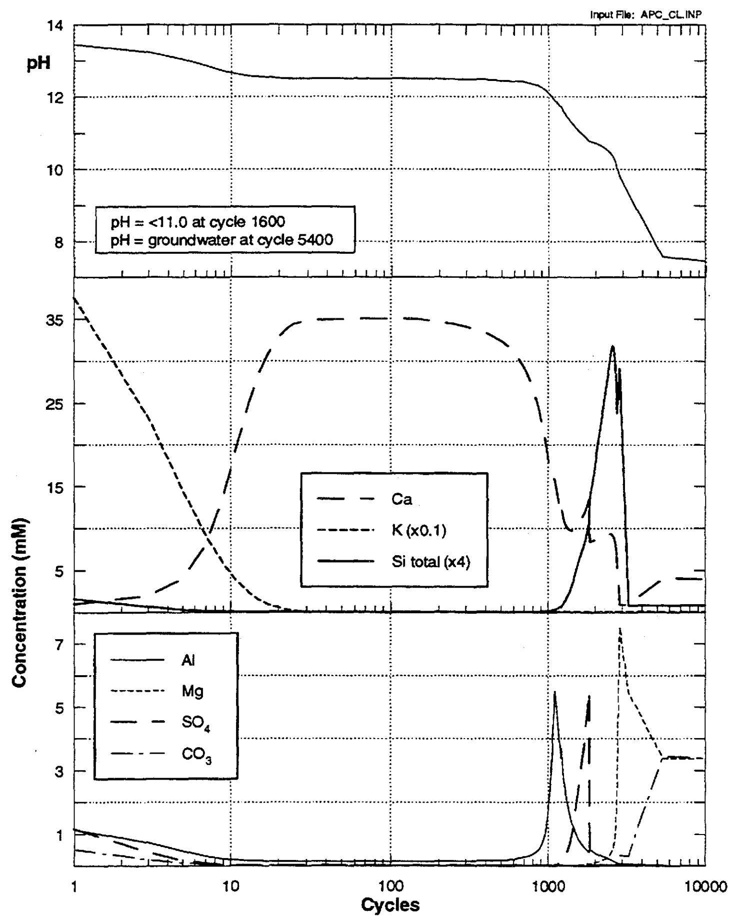

Figure B-6: Results of the cement degradation modelling for cavern lining cement (average Swiss Portland cement) in Wellenberg NaCl water

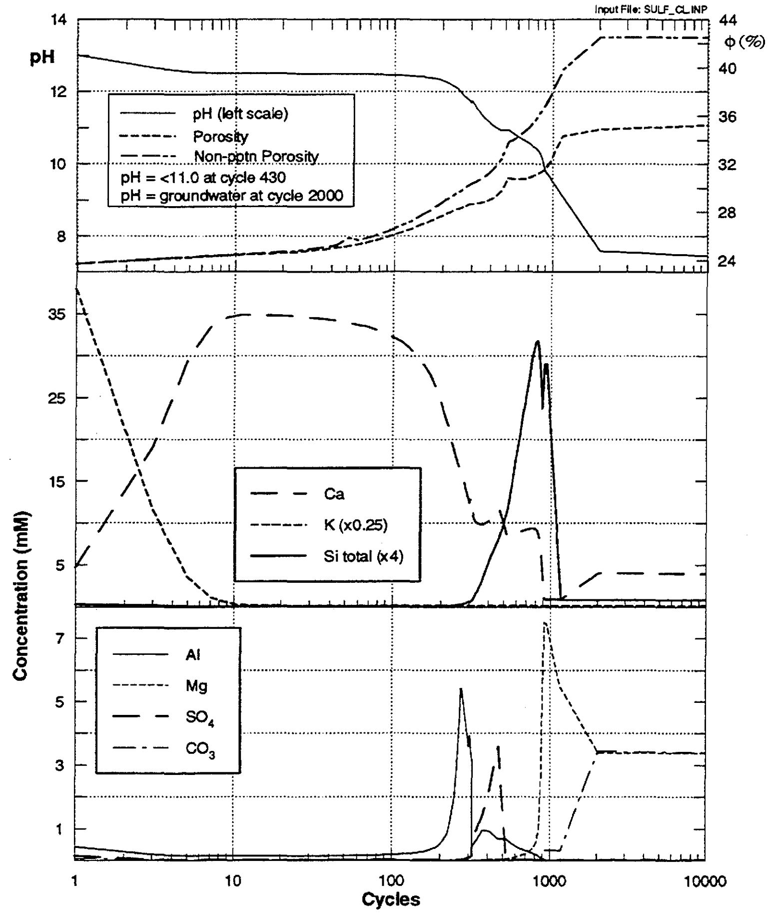

Figure B-7: Results of the cement degradation modelling for cavern backfill cement (Sulfacem modelled with 24% concrete porosity) in Wellenberg NaCl water. Non-precipitation (non-pptn) porosity is the normal porosity plus the porosity filled by secondary (precipitated) minerals.

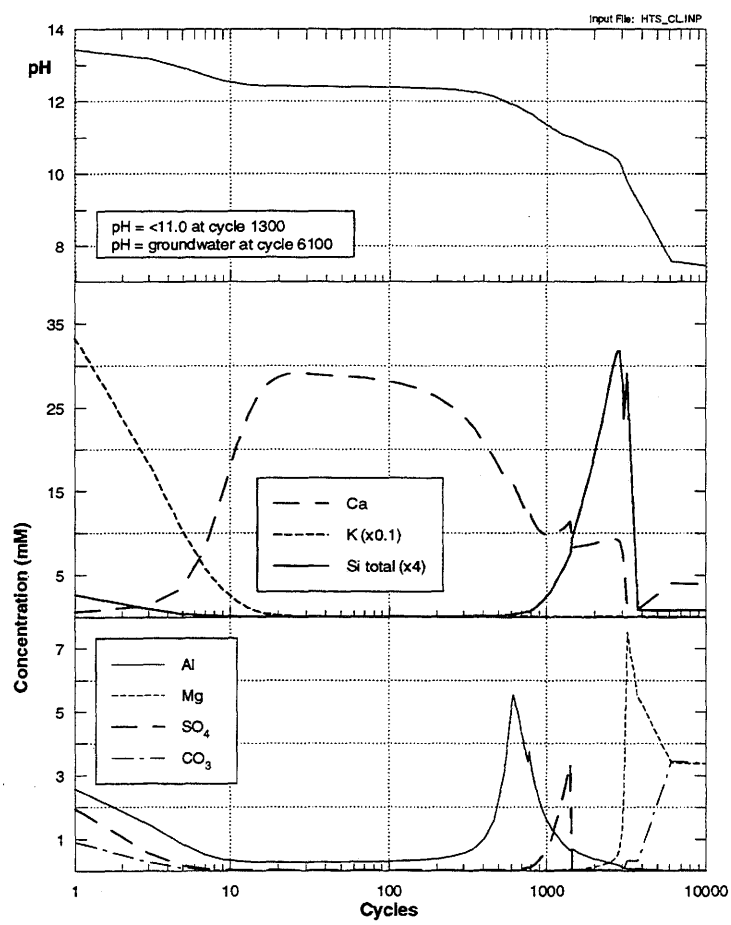

Figure B-8: Results of the cement degradation modelling for cavern type 1 waste cement (HTS plus trass) in Wellenberg NaCl water

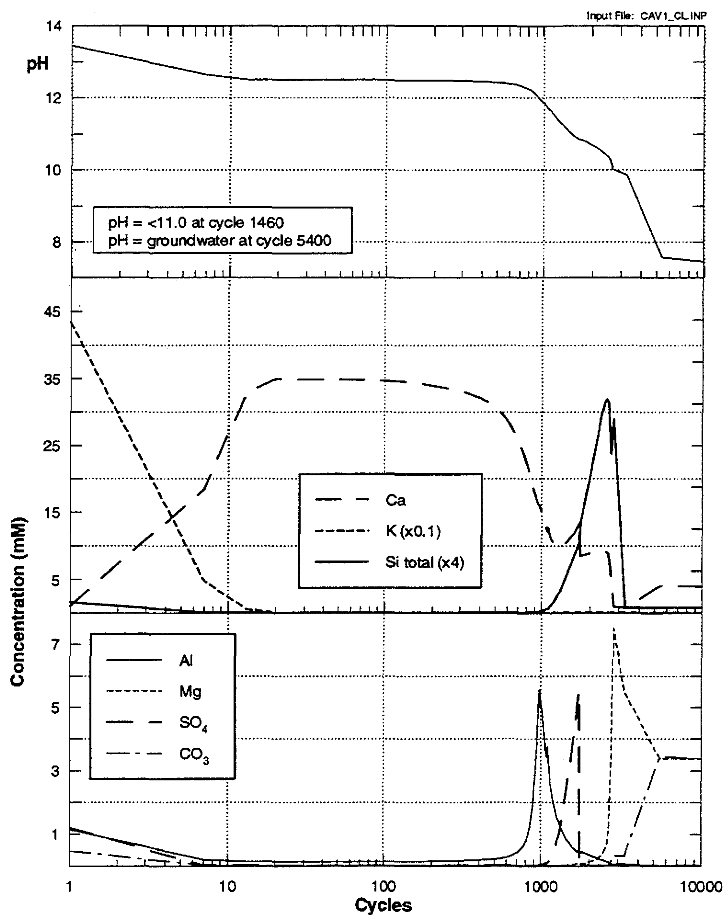

Figure B-9: Results of the cement degradation modelling for cavern type 1 container walls cement (Sulfacem with minimum porosity) in Wellenberg NaCl water.

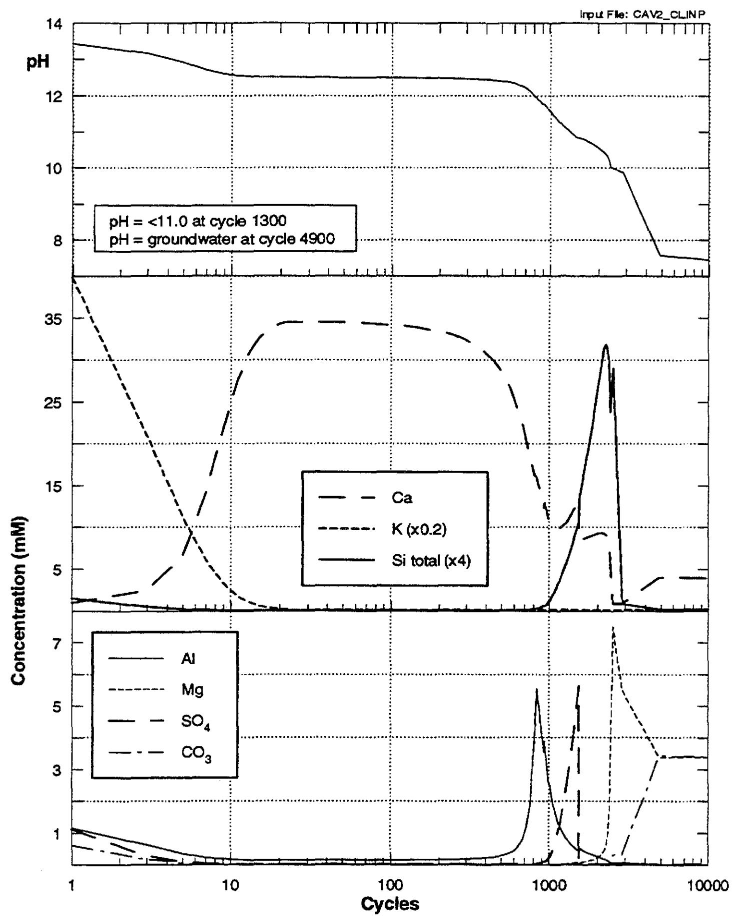

Fig. B-10: Results of the cement degradation modelling for cavern type 2 container infill and walls cement (ordinary Portland cement) in Wellenberg NaCl water.

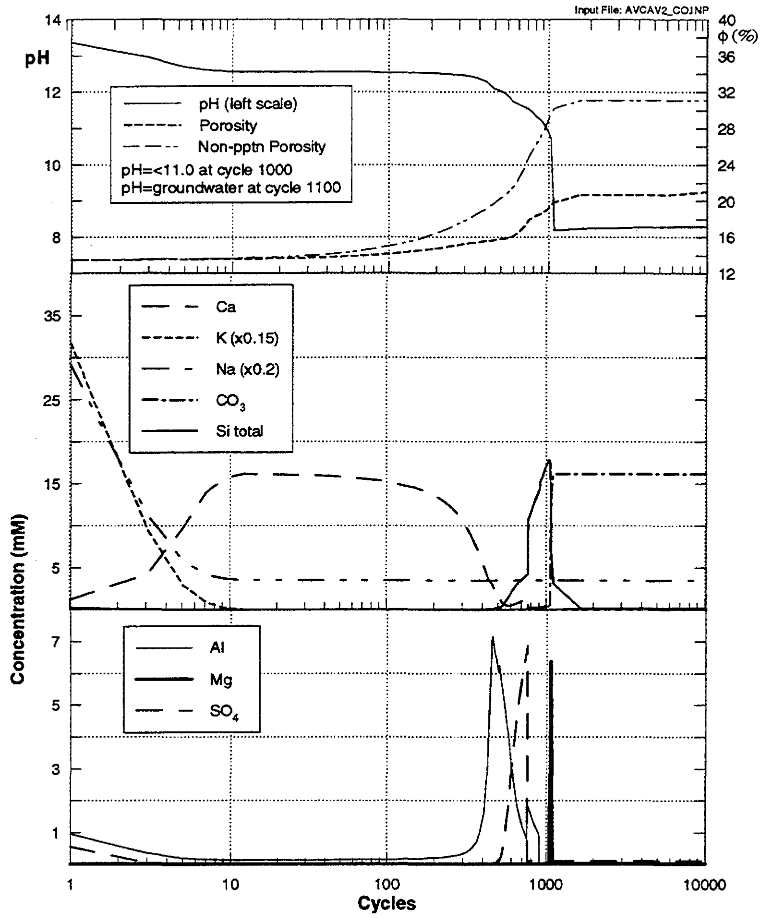

Fig. B-11: Results of the cement degradation modelling for averaged cavern type 2 cement in Wellenberg $NaHCO_3$ water. Non-precipitation porosity is normal porosity plus the porosity filled by secondary (precipitated) minerals.

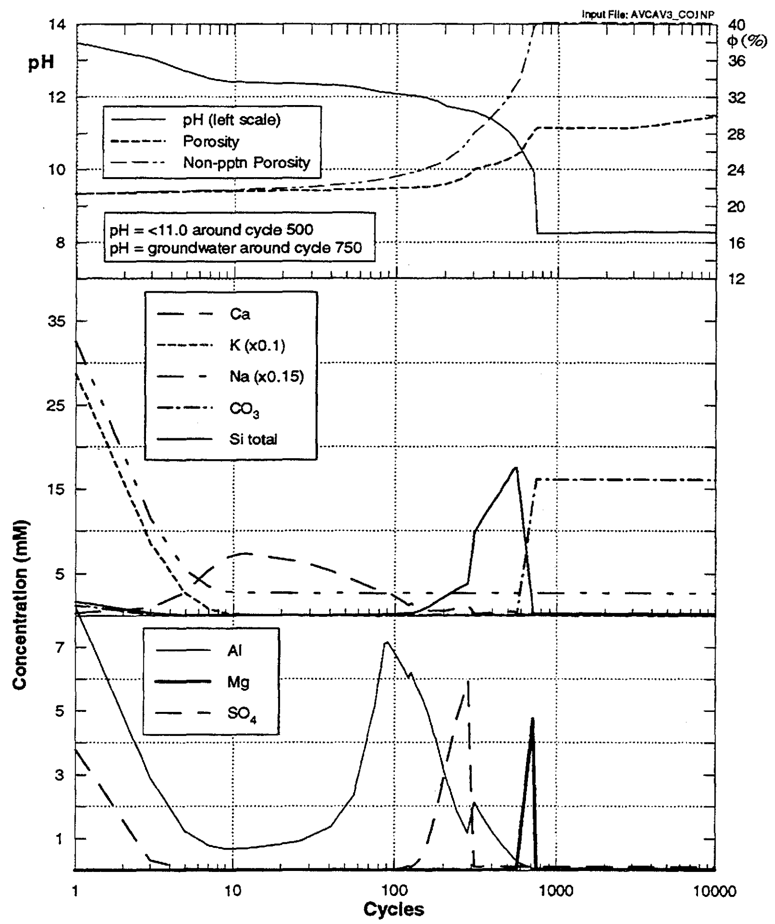

Fig. B-12: Results of the cement degradation modelling for averaged cavern type 3 cement in Wellenberg $NaHCO_3$ water.

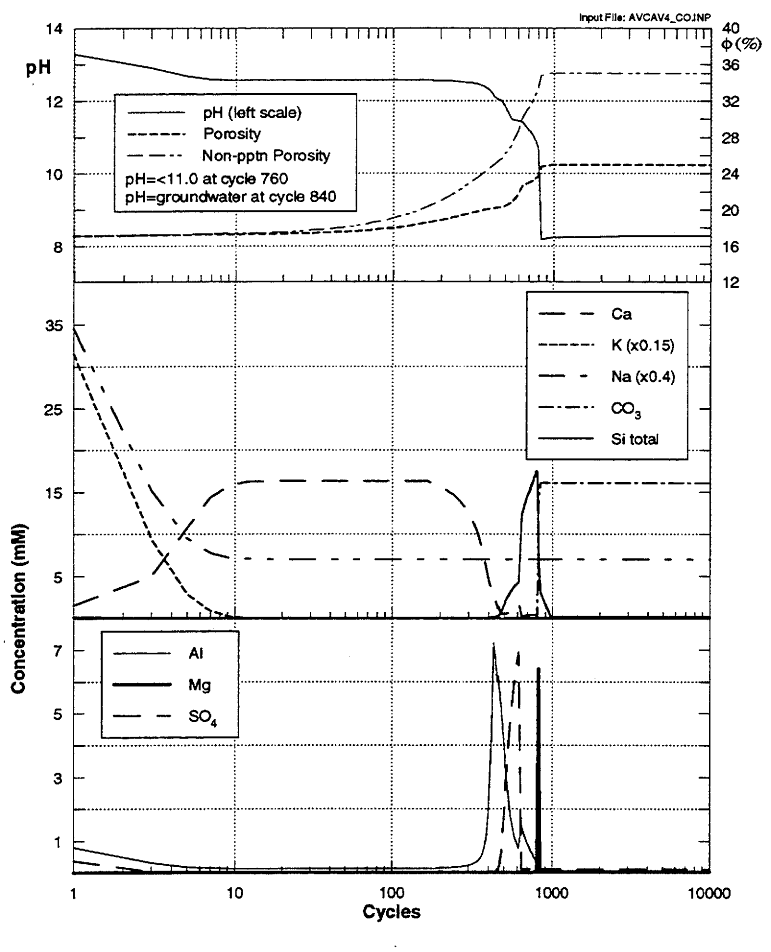

Fig. B-13: Results of the cement degradation modelling for averaged cavern type 4 cement in Wellenberg $NaHCO_3$ water.

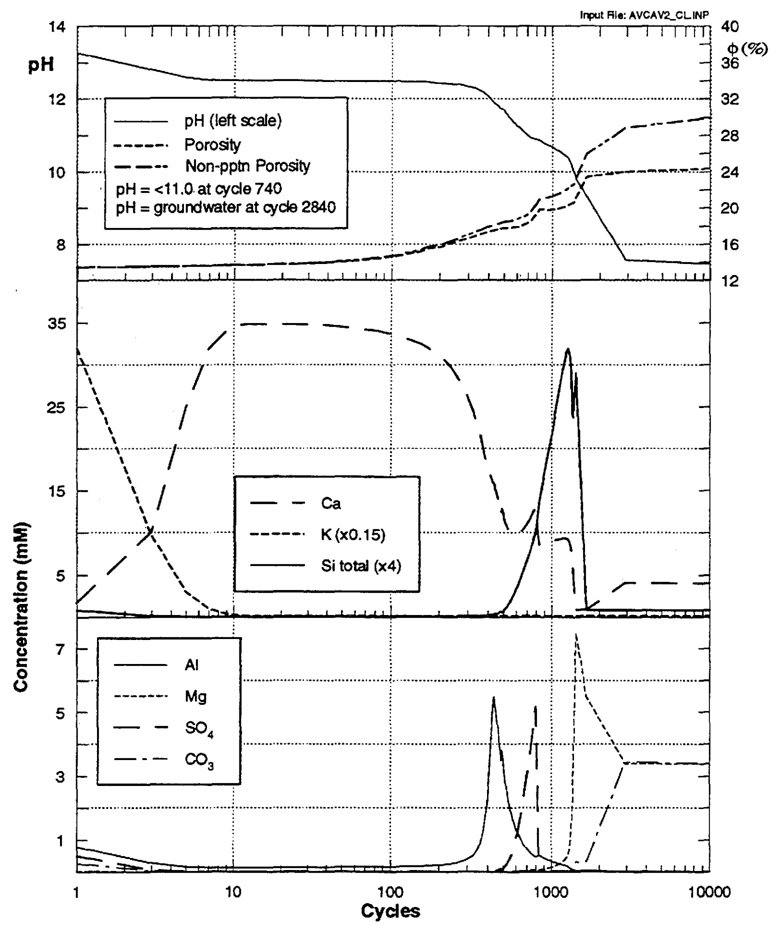

Fig. B-14: Results of the cement degradation modelling for averaged cavern type 2 cement in Wellenberg NaCl water.

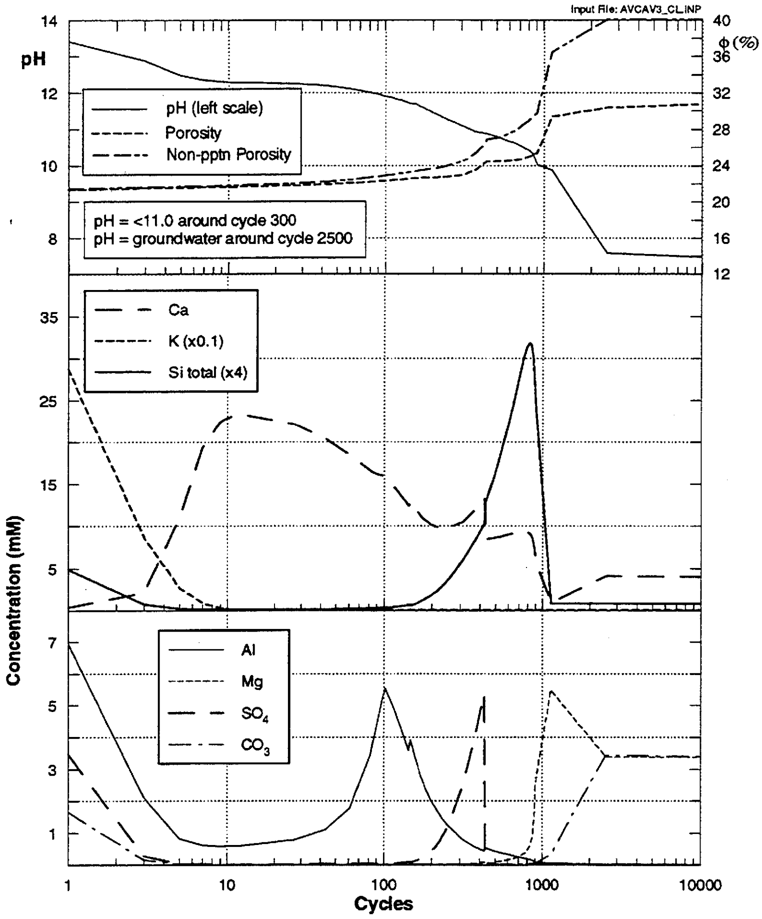

Fig. B-15: Results of the cement degradation modelling for averaged cavern type 3 cement in Wellenberg NaCl water.

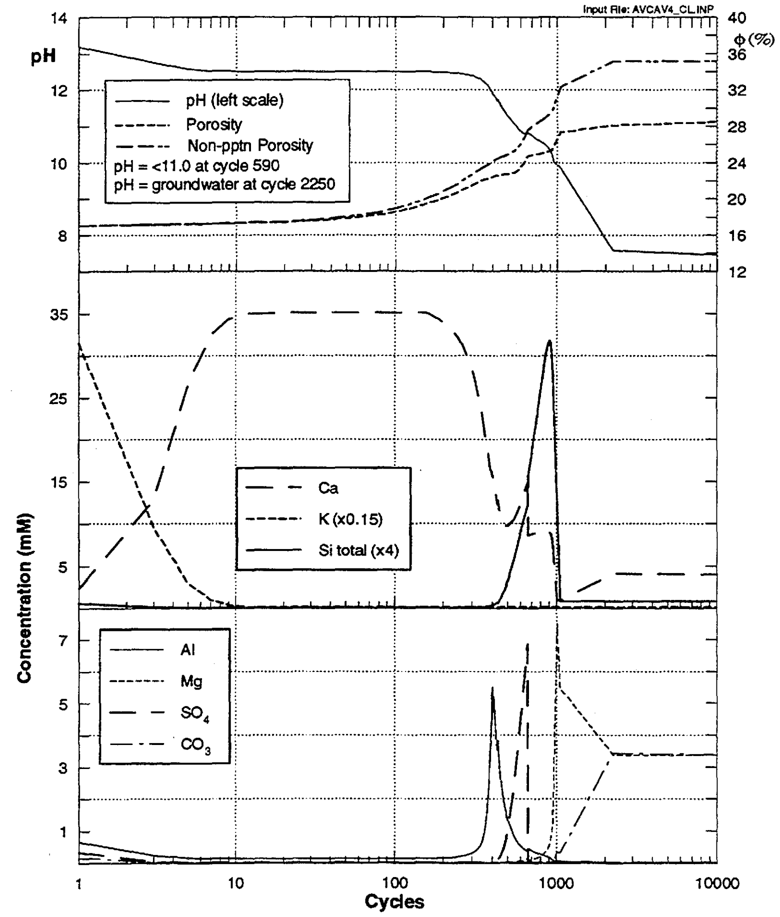

Fig. B-16: Results of the cement degradation modelling for averaged cavern type 4 cement in Wellenberg NaCl water.

APPENDIX C

ADDITIONS TO THE BERNER CEMENT DEGRADATION MODEL - CONSIDERATION OF THE EXPERIMENTAL AND THERMODYNAMIC DATA.

C.1 INTRODUCTION

The current cement degradation model (BERNER 1990) describes the incongruent dissolution of the calcium-silicate-hydrate (CSH) gel phase of the cement. Magnesium, in the form of brucite ($Mg(OH)_2$ or MH), sodium- and potassium hydroxide are included but other significant phase are omitted. To try to improve on the modelling of BERNER (1990), additional phases are needed to better describe the cement composition. The work presented here is the derivation of solubility constants ($LogK_{sp}$) from experimental data for three additional phases. The most important of these new phases are hydrogarnet (C_3AH_6) and ettringite ($C_6A\bar{s}_3H_{32}$), allowing the incorporation of Al and sulphate into the model. The third phase considered is hydrotalcite (M_4AH_{10}), an alternative host for Mg in the model. As the work was carried out within tight deadlines, the thermodynamic constants derived represent the best which could be done within the time available (< 1 month) using existing, albeit mostly recent, experimental data. Uncertainties in the derived values are discussed in terms of their influence on the resulting model.

A recently published experimental study by ATKINS et al. (1992) provides both a good source of data and, from the compatibility experiments, independent solution compositions against which the model can be checked. Solubility constants for the three new phases were derived from solution compositions for the pure phase dissolved in distilled water at 24°C. The solubility constant for a phase which dissolves congruently (i.e. the resulting solution composition reflects the proportions of the components in the solid) is the product of the activities of the component species in solutions raised to the power of their reaction coefficient. That is, for the reaction

$$AB_2 \Leftrightarrow A^{2+} + 2B^-$$

The solubility constant $K_{sp} = (A^{2+}) \cdot (B^-)^2$ where ( ) denotes the activity of a species.

The activities of species in solution were calculated from solution compositions using the speciation code EQ3NR (WOLERY 1983) but using the thermodynamic constants from the Nagra thermochemical database (PEARSON & BERNER 1991; PEARSON et al. 1992). This was to ensure that the resultant solubility constants were compatible with the existing database.

C.2 HYDROGARNET

Hydrogarnet is generally considered to dissolve congruently (e.g. LEA 1970). The $LogK_{sp}$ for hydrogarnet is derived by considering its dissolution according to the reaction:

$$C_3AH_6 \Leftrightarrow 3Ca^{2+} + 2Al^{3+} + 12OH^-$$

$$LogK_{sp} = Log((Ca^{2+})^3 \cdot (Al^{3+})^2 \cdot (OH^-)^{12})$$

The experimental data for hydrogarnet solubility from ATKINS et al. (1992) are given in Table C-1. The solution compositions show considerable charge imbalances and also deviations from the ideal Ca:Al:OH ratio of 3:2:12 in some cases. For these reasons, analyses 3 and 6 were not used in the calculation of solubility product although they are included in Table C-2 for completeness. In addition, there appears to be a systematic variation in Ca:Al ratio and in the charge imbalance through the series of experiments (which are the sequential immersions of the same hydrogarnet sample in distilled water at 25°C). It is uncertain whether this is coincidental experimental error, the influence of a contaminant phase, e.g. portlandite (CH), in small amounts which is preferentially dissolved, or slightly incongruent behaviour.

The solution should be balanced with respect to charge, thus the charge imbalances must result from either errors in the solution analysis or the presence of impurities. The level of the charge imbalances (millimolar) makes it unlikely that they could result from impurities in such a simple system constructed from high purity reagents. It is more likely that they arise from analytical errors, particularly in Al and OH because of the methods used for these analyses (ATKINS et al. 1992).

Based on this assumption, the concentration of Al or OH can be adjusted to give charge balanced solution compositions, and solubility products determined from these. Table C-2 shows the range of $LogK_{sp}$ calculated from

a) the charge unbalanced solution compositions;

b) solution compositions assuming all the error is in the OH concentrations;

c) solution compositions assuming all the error is in the Al concentration.

Table C-1: Solubility of hydrogarnet in pure water at 25°C ($mmol/dm^3$)

Analysis Number	Ca	Al_{total}	OH	Ca:Al	Ca:OH	Charge Imbalance
1	7.43	4.40	23.4	1.69	0.32	+4.66
2	7.31	4.81	27.0	1.52	0.27	+ 2.05
3	5.11	5.20	23.3	0.98	0.22	+ 2.52
4	5.16	3.80	23.4	1.36	0.22	-1.68
5	6.49	4.80	29.6	1.35	0.22	-2.22
6	5.33	4.40	28.1	1.21	0.19	-4.24
			Ideal:	1.5	0.25	

Experimental data from ATKINS et al. 1992.

Analysis Number	$LogK_{sp}$ Un-balanced	Al-balanced	OH-balanced
1	-87.75	-86.78	-86.91
2	-87.21	-86.84	-86.76
3	-89.42	-88.37	-88.13
4	-87.67	-88.05	-88.09
5	-86.85	-87.25	-87.29
6	-87.12	-87.96	-88.17
Mean*	-87.37	-87.23	-87.26

Unbalanced: $LogK_{sp}$ calculated with existing charge imbalance
Al-balanced: $LogK_{sp}$ calculated using OH^- to balance charge
OH-balanced: $LogK_{sp}$ calculated using Al^{3+} to balance charge
* Mean value of Analyses 1,2 4 and 5 only

Table C-2: Hydrogarnet $LogK_{sp}$ calculated from the experimental data of ATKINS et al. (1992)

The solubility products derived from charge balanced solutions should be more reliable than those from the unbalanced solutions except that it is not known with which ion(s) the analytical error lies. However, from Table C-2 it is clear that it matters little which ion is used for charge balancing (in fact, if the charge imbalance is removed by adjusting the Ca concentration, the resulting solubility products are also very close to those given in columns B and C in the table) as the differences between balanced and unbalanced solution solubility products are larger than between those calculated by balancing on Al or OH. Thus the $LogK_{sp}$ is relatively insensitive to the ion to charge balance. Charge balancing the solution compositions can also improve the Ca:Al or Ca:OH ratios (one or the other is improved as the solution is balanced by adjusting Al or OH, respectively). The mean of the solubility products from charge balanced solutions with improved ionic ratio (one for each analysis) is -87.3 and is the favoured $LogK_{sp}$ value for the dataset of ATKINS et al. (1992). It compares with their value of -86.8, calculated using the Aberdeen University MINEQL database. Table C-3 lists other values from the literature for hydrogarnet solubility constants.

ATKINS et al. (1992) observe that the experiments of D'ANS & EICK show signs of disequilibrium when the solution used was undersaturated with respect to portlandite. They suggest that only the experiment in which the solution was saturated with respect to portlandite achieved equilibrium and thus, the only reliable $LogK_{sp}$ is the highest value calculated (-87.2). They cite another experimental study (JONES & ROBERTS 1962) which confirms this higher value. The calculated values from REARDON, VIEILLARD & RASSINEUX and KOMURKA & SCHEIBER are all based on different compilations of thermodynamic data and, as such, are probably less reliable than the experimentally determined values. However, it is interesting to note that two of these values are very close to the favoured experimental value around -87.2.

REARDON (1990)	-86.6	Theoretical derivation (ΔG_f etc.)
VIEILLARD & RASSINEUX (1992)	-86.9	Theoretical derivation
KOMURKA & SCHEIBER (1989)	-88.4	Theoretical derivation
D'ANS & EICK (1953)	-87.2 to -89.8	Experimental derivation
ATKINS et al. (1992)	-86.8	Experimental derivation
This study	-87.2	Experimental derivation

Table C-3: $LogK_{sp}$ for hydrogarnet dissolution at 25°C

From consideration of the foregoing hydrogarnet solubility products, a value of -87.2 was chosen as the best fit with the most reliable data. This value was tested using the results of the compatibility experiments of ATKINS et al. (1992). Table C-4 shows the comparison of the experimental solution composition with the model prediction for hydrogarnet in portlandite saturated solution and also in 0.4M NaOH solution, although in this case the experimental values are not very reliable as portlandite and C_4AH_{13} were observed to precipitate.

Table C-4: Comparison of experiments and model predictions for hydrogarnet dissolution (mmol/dm^3)

	Ca	**Al**	**OH**	**pH**
HG in water				
Experimental*	6.60	4.45	25.9	11.84
Model Prediction	7.00	4.67	28.4	11.98
HG in CH saturated water				
Experimental	16.6	0.18		
Model Prediction	20.6	0.12	36.7	12.48
HG in 0.4M NaOH solution				
Experimental**	0.78	2.07		
Model Prediction	1.01	1.19	40.5	13.4

* Average of runs 1, 2, 4 and 5 from ATKINS et al. (1992)

** CH and C_4AH_{13} precipitated during this run.

C.3 ETTRINGITE

As with hydrogarnet, the experimental results of ATKINS et al. (1992) are a starting point for the calculation of ettringite $LogK_{sp}$. The experimental results are given in Table C-5 with ionic ratios. There are large divergences from ideal ionic ratios in solution in all experiments. This observation and the existence of large charge imbalances in the solution analyses indicate that these data must be used with care. The $LogK_{sp}$ for ettringite is determined from the reaction:

$$C_6A\bar{s}_3H_{32} \Leftrightarrow 6Ca^{2+} + 2Al^{3+} + 3SO_4^{2-} + 12OH^-$$

$$LogK_{sp} = Log((Ca^{2+})^6 \cdot (Al^{3+}) \cdot (SO_4^{2-})^3 \cdot (OH^-)^{12})$$

In fact, only results from experiments 3 to 6 were used to calculated $LogK_{sp}$ (Table C-6). Even so, charge imbalances are so large (> ±1.0 mmol/dm^3) that it is often not possible to calculate a charge-balanced solubility product using single cations or anions except for Ca. Where charge-balanced $LogK_{sp}$'s can be calculated they show a wide range of values as different ions are used to charge-balance the solution (e.g. Analysis number 4). It should also be noted that, in some cases, the adjustment of the solution composition to satisfy charge balancing criteria results in solution ionic ratios even further from the ideal values. Where charge balancing results in a significantly worse ionic ratios, the solubility products are given in parentheses (Table C-6).

The wider range of solubility products for ettringite, compared to hydrogarnet, make it more difficult to select a precise value; the experimental work of ATKINS et al. (1992) indicates that it probably lies in the range -110 to -112 (ATKINS et al. calculate

Table C-5: Experimental determinations of the solubility of ettringite in pure water at 25°C (mmol/dm^3)

Analysis Number	Ca	Al_{total}	SO_4	OH	Ca:Al	Ca:SO_4	Charge Imbalance
1(A)	2.67	0.29	1.68	2.90	9.21	1.59	-0.05
2(A)	2.00	0.41	1.20	2.60	4.88	1.67	+0.23
3(A)	2.29	0.54	0.98	3.10	4.24	2.34	+1.14
4(A)	1.82	0.65	1.27	4.20	2.8	1.43	-1.15
5(A)	1.43	0.41	1.00	3.70	3.49	1.43	-2.11
6(A)	1.25	0.41	1.00	3.70	3.05	1.25	-1.97
7(A)	1.21	0.59	1.04	3.30	2.05	1.16	-1.19
8(A)	1.97	0.37	0.97	3.00	5.32	2.03	+0.11
9(Z)	2.53	0.714	1.30	3.87*	3.54	1.94	
				Ideal ratio:	3.0	2.0	

(A) data from ATKINS et al.1992
(Z) data from ZHANG et al. 1980
* (OH) calculated from charge balance

Analysis Number	$LogK_{sp}$				
	Un-balanced	Ca-balanced	Al-balanced	SO_4-balanced	OH-balanced
3(A)	-112.2	-112.8	(-111.6)	-111.8	-110.8
4(A)	-111.4	-110.8	(-116.4)	-108.0	(-113.5)
5(A)	-111.7	-	-	-	-114.6
6(A)	-112.4	-	-	(-117.4)	-117.7
9(Z)	-	-	-	-	-110.4

Unbalanced: $LogK_{sp}$calculated with existing charge imbalance
Ca-balanced: $LogK_{sp}$ calculated using Ca^{2+} to adjust solution charge imbalance
Al-balanced: $LogK_{sp}$ calculated using Al^{3+} to adjust solution charge imbalance
SO_4-balanced: $LogK_{sp}$ calculated using SO_4^{2-} to adjust solution charge imbalance
OH-balanced: $LogK_{sp}$ calculated using OH^- to adjust solution charge imbalance
(A) Solution compositions from ATKINS et al.1992
(Z) Solution composition from ZHANG et al.1980

Table C-6: $LogK_{sp}$ for ettringite calculated from the experimental data

REARDON (1990)	-109.8	Theoretical derivation (ΔG_f etc.)
VIEILLARD & RASSINEUX (1992)	-106.7	Theoretical derivation
KOMURKA & SCHEIBER (1989)	-100.4	Theoretical derivation
LEA (1970)	-108.5	Experimental*
ATKINS et al. (1992)	-111.3	Experimental derivation
This study	-111.0	Experimental derivation

* LEA states that "in a lime solution containing 0.53g CaO per litre, [ettringite] dissolves to give a solution containing only **about** 0.01g SO_3 and 0.008g Al_2O_3 per litre" - hardly a precise experimental determination.

Table C-7: Values from the literature for $LogK_{sp}$ of ettringite dissolution at 25°C.

a value of -111.3). A value of -111.0 was used in the comparison with the compatibility experiments (Table C-8) as it gives the best fit with data from these experiments.

	Ca	Al_{total}	SO_4
Ettringite + Portlandite			
Experimental*	16.51	0.043	<0.01
Model prediction	20.58	0.016	0.023
Ettringite + Hydrogarnet			
Experimental*	5.11	1.54	<0.01
Model prediction	7.01	4.67	0.008

* Experimental data from ATKINS et al.1992

Table C-8: Comparison of experiments and model predictions for ettringite dissolution at 25°C

C.4 HYDROTALCITE

Hydrotalcite presents a problem, having a varying composition depending on the phase assemblage

For Mg/Al<4.0 in the presence of AH the composition is M_4AH_{10}
For Mg/Al = 4.0 to 6.0 the composition is $M_{4\text{-}6}AH_{10\text{-}13}$
For Mg/Al>6.0 in the presence of MH the composition is M_6AH_{13}

(MASCOLO & MARINO,1980)

In the experiments of ATKINS et al. (1992), the two endmember compositions of hydrotalcite were used. However, the presence of aluminium hydroxide (AH) or brucite (MH) distorted the solution compositions. For example, the presence of MH lowers the concentration of Al relative to pure hydrotalcite in water. ATKINS et al. also state that saturation indices show the MH is actively leached from the high-Mg hydrotalcite. Although they derive a solubility product (which assumes congruent dissolution) for the low Mg hydrotalcite (M_4AH_{10}) from the results of two analyses, they note inconsistencies which arise when the water/solid ratio in the experiment is increased. They do not give details of the increase in water/solid ratio but, as can be seen in Table C-9, the Mg concentration doubles while that of Al halves. This could be explained by leaching of Mg from the low Mg hydrotalcite also; by precipitation of an Al phase (traces of AH were detected by XRD); or failure of the experiment to reach equilibrium.

Using the data from Analyses 3 and 4 of ATKINS et al. (1992) (Table C-9) a $LogK_{sp}$ of -122.2 can be determined from the relationship:

$$M_4AH_{10} \Leftrightarrow 4Mg^{2+} + 2Al^{3+} + 140H^{-}$$

$$LogK_{sp} = Log((Mg)^4 \cdot (Al^{3+})^2 \cdot (OH^-)^{14})$$

However, this solubility product does not duplicate the results of the compatibility experiments at high pH (Table C-10) which, in any case show significant incongruency in the solution compositions. ATKINS et al. suggest that the solubility can be better approximated by modelling hydrotalcite as a combination of brucite and aluminium hydroxide with two solubility products - one for AH dissolution and the other for MH. They use their experimental data to derive values for these solubility products. The calculated values are $LogK_{sp}(MH) = 19.9$ and $LogK_{sp}(AH) = 6.84^{*}$. These contrast with the MINEQL/Nagra database values of 16.8 and 8.11 respectively. Predictions using both these sets of values are compared with the experimental results in Table C-10.

Table C-9: The solubility of hydrotalcite (M_4AH_{10}) in water at 25°C (mmol/dm^3)

Analysis Number	**Mg**	**Al_{total}**	**OH/pH**
2	0.003	0.111	0.342
3	0.033	0.014	pH = 9.3
4	0.035	0.010	pH = 9.3
Increased water/solid ratio*			
5	0.060	0.008	-
6	0.072	<0.005	-

Experimental data from ATKINS et al. 1992
* no details of amount of increase given in ATKINS et al. (1992)

To describe hydrotalcite in terms of two solubility products introduces practical problems insofar as the DISSOLVE program already treats the incongruently soluble CSH as a pair of independent model phases. To introduce a second incongruently soluble solid represented by another pair of model phases would cause mathematical problems at runtime. To avoid such problems would require significant recoding in the DISSOLVE program. Such effort was not possible due to time constraints and alternative options were sought. At pH 11 and above, Al in solution is dominated by hydrogarnet dissolution (e.g. M_4AH_{10} + HG, Table C-10), thus it is possible to model Mg behaviour in the degrading cement porewater in terms of MH alone. The MINEQL/Nagra solubility product for brucite (16.8) was used as there is little evidence to suggest that the $LogK_{sp}$ given by ATKINS et al. (1992) better reproduces the Mg concentrations in the compatibility experiments. The higher pH (ca. 12) predicted for the assemblage hydrotalcite + hydrogarnet is relatively unimportant as the CSH phase still influences the pH to around 11 so the effect will be to increase the concentrations of Mg and Al for this assemblage. The lower pH, both experimental and predicted, for hydrotalcite + AH mean that, in practical terms, this assemblage is outside the pH range of interest (pH > 11). Although careful choice of solubility products for AH and

---

* $Mg(OH)_2 + 2H^+ \Leftrightarrow Mg^{2+} + 2H_2O$ $\quad$ $LogK_{sp(MH)} = Log\,(Mg^{2+}) + 2pH$

$Al(OH)_3 + 3H^+ \Leftrightarrow Al^{3+} + 3H_2O$ $\quad$ $LogK_{sp(AH)} = Log\,(Al^{3+}) + 3pH$

MH may allow modelling of hydrotalcite incongruent dissolution to better replicate the experimental results, the actual benefit over the simple proposal given here may not justify the effort needed.

Table C-10: Comparison of experimental results and model predictions for the solubility of hydrotalcite ($mmol/dm^3$)

	Ca	Al_{total}	Mg	pH
M_4AH_{10} + CH				
Experimental	16.72	0.066	<0.002	11.8
ATKINS et al. $LogK_{sp}$	19.0	3.6×10^{-5}	< 2×10^{-5}	12.4
MH + AH (ATKINS et al.)	24.0	0.170	0.012	12.4
MH + AH (This study)	17.2	0.18	6.0×10^{-5}	12.45
M_4AH_{10} + 0.4M NaOH				
Experimental	-	1.10	<0.004	-
ATKINS et al. $LogK_{sp}$	-	1.5×10^{-5}	3.0×10^{-5}	13.39
MH + AH (ATKINS et al.)	-	1.82	0.08	13.41
MH + AH (This study)	-	1.84	6.7×10^{-5}	13.41
M_4AH_{10}+ AH				
Experimental	-	0.004	0.045	9.1
ATKINS et al. $LogK_{sp}$	-	0.005	0.020	9.6
MH + AH (ATKINS et al.)	-	0.08	2.5	11.4
MH + AH (This study)	-	0.065	0.15	10.3
M_4AH_{10} + HG				
Experimental	4.6	2.5	<0.002	11.0
ATKINS et al. $LogK_{sp}$	5.75	3.8	8.1×10^{-7}	11.8
MH + AH (This study)	7.3	3.02	0.0004	11.9
MH alone (This study)	7.0	4.6	0.0006	11.8

C.5 SUMMARY

Solubility products for hydrogarnet and ettringite were derived from the experimental data of ATKINS et al. (1992). The resulting values are

Hydrogarnet $C_3AH_6 \Leftrightarrow 3Ca^{2+} + 2Al^{3+} + 12OH^-$ $LogK_{sp} = -87.2$

Ettringite $C_6A\bar{S}_3H_{32} \Leftrightarrow 6Ca^{2+} + 2Al^{3+} + 3SO_4^{2-} + 12OH^-$ $LogK_{sp} = -111.0$

The magnesium phase hydrotalcite has variable composition and appears to dissolve incongruently, at least under some (high pH) conditions. Consequently the single $LogK_{sp}$ suggested by ATKINS et al. (1992) was considered unrealistic. Describing hydrotalcite dissolution in terms of two model phases (AH and MH) with independent solubilities has not been implemented due to time constraints and the necessity of significant software amendments with this option. Instead a single (brucite) solubility product is used to model Mg in the pore fluid; Al is assumed to be dominated by hydrogarnet dissolution.

Hydrotalcite (M_4AH_{10}) $\quad$ $LogK_{sp(MH)} = -16.8$

These solubility constants are by no means a final answer but interim values in limited time from a restricted dataset. Further work may be necessary to improve on them. However, throughout the most important part of the repository lifetime, the high pH porewater interval, pH is dominated by the CSH phase. The hydrogarnet and ettringite become important only as pH falls significantly below 12. The influence of hydrotalcite is even later when the pH is below 11. Hence, the model is relatively insensitive, in terms of both the porewater pH and the duration of the high pH porewater interval, to changes in solubility constants for these minor phases. Their usefulness is in providing a more complete description of the chemical environment and, potentially, a better understanding of secondary mineral precipitation.